

103

FUMAROLIC ALTERATION OF BASALT
ON MAUNA ULU,
KILAUEA VOLCANO, HAWAII

by
CATHERINE ANNE MATHEWS

Submitted to the Department of Geology
in Partial Fulfilment of the Requirements
for the Degree
Honours Bachelor of Science

McMaster University

April 1983

Honours Bachelor of Science (1983)
(Geology)

McMaster University
Hamilton, Ontario

Title: Fumarolic Alteration of Basalt on Mauna Ulu, Kilauea
Volcano, Hawaii

Author: Catherine Anne Mathews

Supervisor: Dr. Brian J. Burley

Number of Pages: 84,ix

ABSTRACT

Altered olivine tholeiite basalt on Mauna Ulu Volcano, Hawaii was examined petrographically and chemically to determine the mineralogy of the alteration products. Colour plays an important role in determining a general trend of alteration.

The processes involved in the formation of Mauna Ulu have little effect on the alteration. The major influence is the type of volcanic gas and its constant interaction with the basaltic lava over an eight year period. The gas is oxidized as it cools, resulting in a zoning of different alteration products in a variety of colours and compositions.

The major alteration phase was determined to be amorphous opaline silica. Other species present are hematite and sulphur, with minor halides, sulphates and sheet silicate (chlorite).

ACKNOWLEDGEMENTS

I would like to thank Dr. Brian J. Burley for his support as thesis supervisor through the year, Dr. Paul M. Clifford for the planning involved in the trip to Hawaii, and initiation of the thesis topic. Appreciation is extended to Doug Sweeney and Wayne Gignac, both of whom assisted in the collection of field samples. The following are thanked for their assistance: Len Zwicker for thin section preparation; Ota Mudrock for XRF analysis; Ishmael Hassan for XRD analysis; Abdul Kabir for CIPW norms and Jack Whorwood for photography. Many thanks to Lyndor Office Services for typing the manuscript.

Special thanks are extended to the class of '83, especially the music lovers of Room 308, who made those long nights of writing ...interesting.

Above all, I would like to thank Wayne, for without his support and constant prodding, this thesis would never have been started or completed.

TABLE OF CONTENTS

	<u>Page</u>
Abstract	iii
Acknowledgements	iv
List of Tables	vi
List of Figures	vii
Chapter I - Introduction	1
1.1 - Statement of the Problem	1
1.2 - Location and Accessibility	1
1.3 - Previous Work	2
Chapter II - The Formation of Mauna Ulu	7
Chapter III - Petrology	12
3.1 - Introduction	12
3.2 - Petrographic Study	17
3.3 - Refractive Index Determination	26
3.4 - Alteration Development	33
Chapter IV - Geochemistry	46
4.1 - Introduction	46
4.2 - Major Elements and Component Ratios	47
4.3 - CIPW Norms	58
4.4 - Composition - Volume Relationships	60
Chapter V - Volcanic Gas Compositions	70
Chapter VI - Conclusions	79
6.1 - Summary	79
6.2 - Suggestions for Further Work	80
References	83
Appendix	82

LIST OF TABLES

- 3.1.1 Distinguishing Characteristics of hand samples
- 3.1.2 Generalized zoning pattern of encrustations around volcanic fumaroles (Stoiber & Rose, 1974)
- 3.3.1 Minerals with similar refractive indices as samples 1 and 5
- 4.1.1 X-ray Fluorescence Results (normalized to 100), weight percents of oxides
- 4.2.1 Component Ratios
- 4.3.1 CIPW Norms
- 4.4.1 Specific gravities of samples used for gain-loss determinations (determined by displacement method, Hutchison, 1974)
- 4.4.2 Absolute gains and losses (grams)
- 5.1.1 Chemistry of the sublimate collected above Mauna Ulu's lava fountain in January 1970 (Naughton et al, 1974)
- 5.1.2 Calculated equilibrium composition of major (controlling) gaseous components under various conditions of oxidation and temperature (Naughton et al, 1974)
- 6.1.1 Possible alteration products on Mauna Ulu.

LIST OF FIGURES

- 1.2.1 Kilauea Volcano showing location of Mauna Ulu on East Rift Zone (Hazlett, 1982)
- 1.2.2 Mauna Ulu Volcano. Grey pahoehoe lava in foreground, black aa lava on lower flank; grey pahoehoe lava on upper flank; steam, gases and altered material on summit.
- 1.2.3 Contact between black aa lava in background and grey pahoehoe lava in foreground. Southeast of Mauna Ulu's summit.
- 2.1.0 Aloi-Alae Thermal Area; area of localized lava fountaining, January 1969 (Hazlett, 1982)
- 2.2.0 Mauna Ulu Lava Shield; cessation of activity, August 1974 (Hazlett, 1982)
- 3.1.1 Rock filled crater on Mauna Ulu. Left foreground is altered lava at edge of crater. Depth to floor is about 135 m.
- 3.1.2 Steam issuing from a vent on the inside wall of the crater.
- 3.1.3 Altered lava on Mauna Ulu's summit. Note steam vents in background. Crater is to the left.
- 3.1.4 Altered lava on Mauna Ulu's summit. Note steam and colour of material. Crater is to the left.
- 3.2.1 Large vesicle contains angular shards of the basaltic glass. Note zoning lining interior edges of vesicles. Olivine crystal at left lies in a spherulitic glass matrix (sample 2) (160x).
- 3.2.2 Spherulites (sample 2) (250x)
- 3.2.3 Partial olivine grains with relict crystal outlines (sample 1) (160x)
- 3.2.4 Altered olivine crystals in a plagioclase-rich matrix. Alteration products are iddingsite and commonly iron oxides. (sample 4) (63x)
- 3.2.5 Pale orange to light brown, colloformal-type banding between vesicles (sample 2) (63x)

- 3.2.6 Cut sample showing interior of fairly fresh basalt, and exterior of coloured alteration material. Note growths on surface and infilling of vesicles (near base). (sample 4, top direction to upper left corner, base to lower right corner). (sample is 5.5 cm from top to bottom).
- 3.2.7 Dense matrix of Na-rich plagioclase laths with fine grained olivine and pyroxene. (sample 4) (250x)
- 3.4.1 Coating of white and brown material on surface and within vesicles. (sample 12) (sample is 3 cm across)
- 3.4.2 Fresh ropey pahoehoe, with brown coating starting to fill in rivulets on surface. (sample 5) (sample is 3.5 cm from top to bottom)
- 3.4.3 Underside of fairly fresh vesicular lava. Note coatings within vesicles and brown coating over surface. (sample 7) (sample is 5.5 cm from top to bottom).
- 3.4.4 Cut sample showing minute, vertical growths on upper surface and within vesicles; infilling of vesicles with amorphous material, concretionary texture (especially in lower right section of the sample). (sample 2, surface at the top of the picture, base at the bottom). (sample is 4.5 cm from top to bottom).
- 3.4.5 Sample broken open to reveal its interior. Note yellowish, orange, grey, slightly shiny amorphous material. (sample 9) (sample is 5 cm across)
- 3.4.6 Surface of sample showing white, orange and yellow encrustations. Some globular growths are visible. (sample 15) (sample is 6 cm across)
- 3.4.7 Colourful surface of Mauna Ulu's altered deposits. Note variety of colours and crumbly texture.
- 3.4.8 Surface of sample (note extensive oxidation as compared to Figure 3.4.7) showing botryoidal spheres (sample 2). (sample is 8 cm across)
- 4.2.1 Weight percent (SiO_2) vs sample (M.U. is T.L. Wright's Mauna Ulu basalt)
- 4.2.2 Weight percent (Al_2O_3 , Fe_2O_3) vs sample
- 4.2.3 Weight percent (MgO , CaO) vs sample
- 4.2.4 Weight percent (MnO , P_2O_5) vs sample
- 4.2.5 Weight percent (TiO_2 , Na_2O , K_2O) vs sample
- 4.4.1 Gain and Loss (grams) (SiO_2) vs sample (very mobile)

- 4.4.2 Gain and Loss (grams) (Al_2O_3 , Fe_2O_3 , MgO , CaO) vs sample. (mobile)
- 4.4.3 Gain and Loss (grams) (TiO_2 , Na_2O) vs sample (slightly mobile)
- 4.4.4 Gain and Loss (grams) (K_2O , MnO , P_2O_5) vs sample. (immobile)
- 5.1.1 Calculated equilibrium compositions of compounds of the elements H, O, C, S, Cl, Na, Ca, Mg, Cu present above 10^{-16} mole fraction (Naughton et al, 1974).

CHAPTER I - INTRODUCTION

(1.1) Statement of the Problem

In February - March, 1982, a field trip was taken with the Department of Geology, McMaster University, Hamilton to the Hawaiian Islands. A trip to Kilauea Volcano and Mauna Ulu was undertaken; and this thesis developed as a result of that excursion.

The flanks of Mauna Ulu are comprised of pahoehoe and aa type lavas, but the summit around the volcano's crater is extensively altered and decomposed. There are hot gases and steam emanating from vents on the summit, and it is suggested that the alteration of the lava has resulted from the constant interaction with these gaseous phases.

Initial interest was generated by the obvious contrast between the altered products and the original tholeiitic basalt. Encrustations are colourful, mostly orange, yellow, brown and white; and appear to be partially non-crystalline. Temperatures of vent gases on the summit were not accurately measured but are estimated to be from 100⁰C - 250⁰C.

The main purpose of this study has been to determine what these encrustations are; their mineralogy and chemistry; exactly how they formed; how extensive the alteration has progressed, and predictions for future alteration.

(1.2) Location and Accessibility

Mauna Ulu ("Growing Mountain" in Hawaiian) is a 78 m high basaltic shield volcano built up within a period of five years. It is located on the upper east rift zone of Kilauea

Volcano, Hawaii Island, Hawaii; at approximately $19^{\circ}21.5'$ N latitude and $155^{\circ}12.5'$ W longitude (figure 1.2.1). On a large scale, the volcano's location is somewhat isolated in the Pacific Ocean, yet once on the island of Hawaii, a car, a good pair of hiking boots and an observant eye, are all that is required. Kilauea and Mauna Ulu are located within Hawaii Volcanoes National Park. Pahoehoe and aa lavas are found on the flanks of Mauna Ulu. (figure 1.2.2). Both types of lava are very dangerous to walk across, making the area somewhat inaccessible (figure 1.2.3).

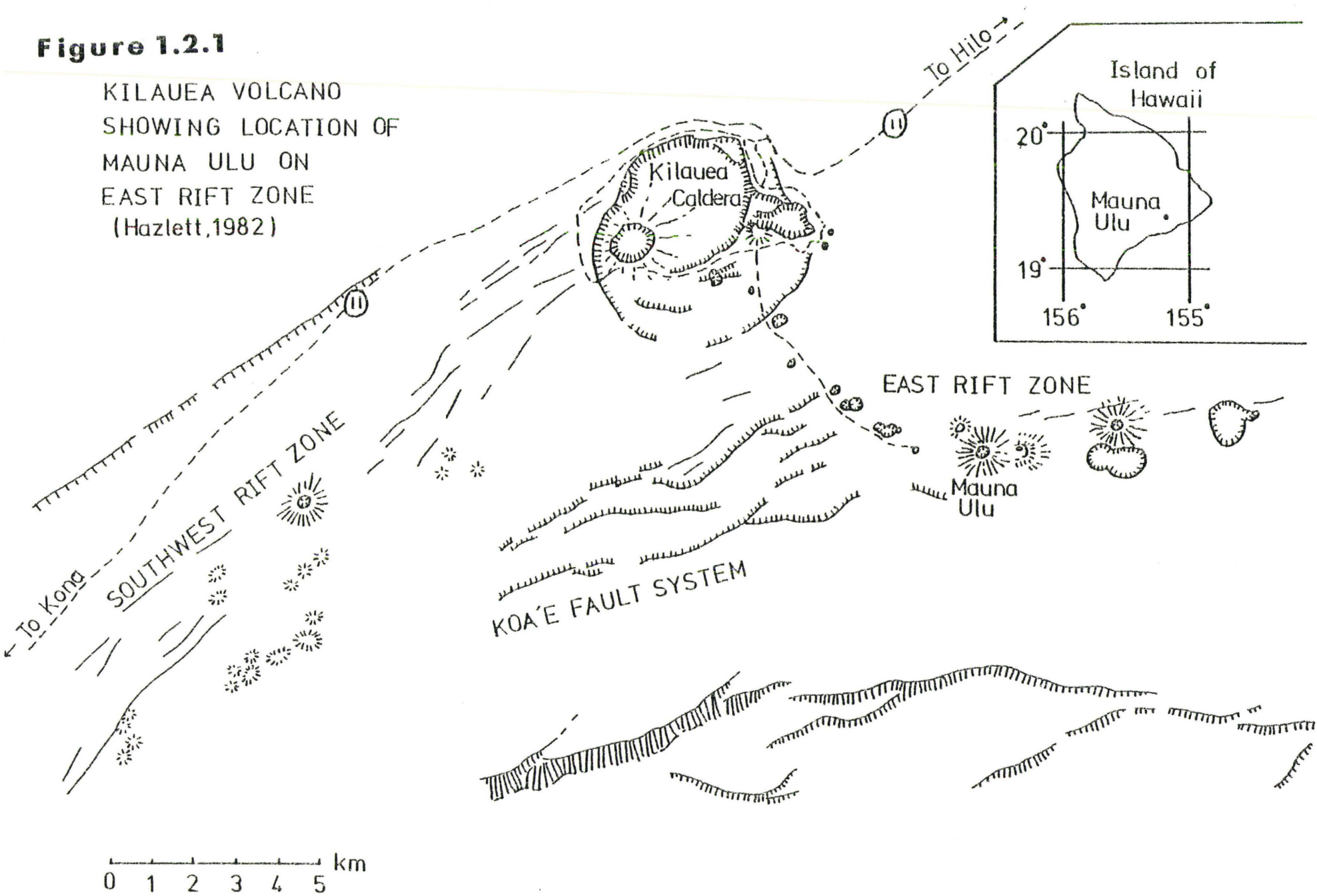
(1.3) Previous Work

The type of study done for this thesis has never before been done on Mauna Ulu, although the volcano has been extensively studied. Mauna Ulu is unique because it is the longest, largest, most varied eruption in Kilauea's recorded history; thus volcanologists, seismologists and even structural geologists have found interests in this volcano. As yet no one has studied the petrology of the altered lava on its summit.

Since the volcano is within Hawaii Volcanoes National Park, persons at the Hawaii Volcano Observatory have carefully studied this volcano's history. They have detailed every eruption and earthquake, and witnessed close up the volcano's activity. Many people have been involved in publishing their findings. In particular; D.A. Swanson has studied magma movements and lava flows; W.A. Duffield compared Mauna Ulu's lava

Figure 1.2.1

KILAUEA VOLCANO
SHOWING LOCATION OF
MAUNA ULU ON
EAST RIFT ZONE
(Hazlett, 1982)



4

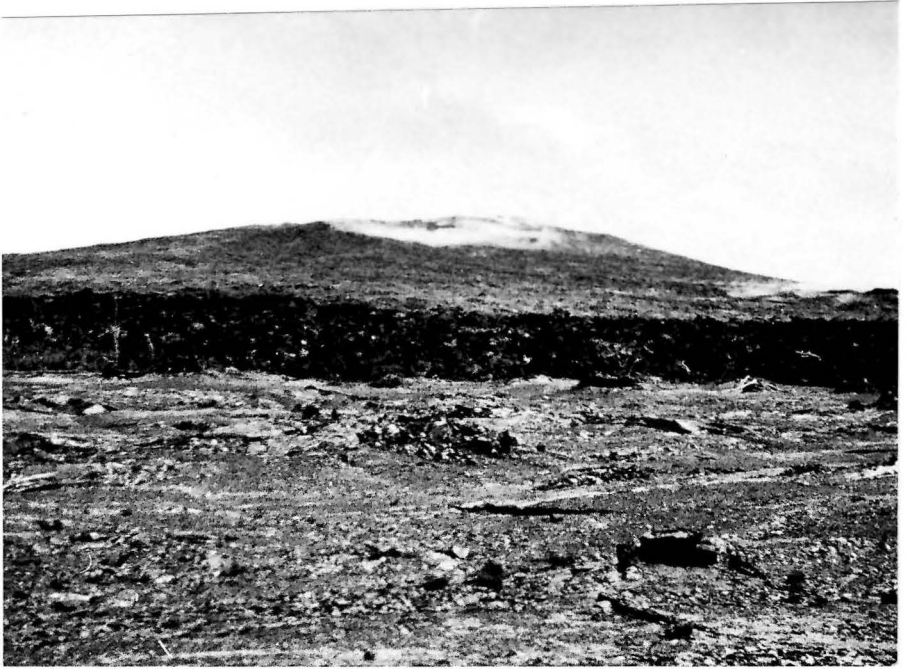
Figure 1.2.2

Mauna Ulu Volcano

Grey pahoehoe lava in foreground; black aa lava on lower flank; grey pahoehoe lava on upper flank; steam, gases and altered material on summit.

Figure 1.2.3

Contact between black aa lava in background and grey pahoehoe lava in foreground. Southeast of Mauna Ulu's summit.



Takes to global plate tectonics, and the study of lava tubes and island growth was done by D.W. Peterson.

When Mount St. Helens erupted in 1980, numerous fumaroles were found in and around the crater. Encrustations similar to those on Mauna Ulu surrounded most of these fumaroles. These were studied by the United States Geological Survey, in particular T.E.C. Keith, D.P. Deltheir and D.R. Pevear.

R.E. Stoiber and W.I. Rose have extensively studied the fumaroles in and around Central American volcanoes. Their work involved over eleven years of research on fourteen different volcanoes.

Volcanic gas analyses at Kilauea have been investigated principally by J.J. Naughton and T.M. Gerlach at the Hawaii Volcano Observatory and the Hawaii Institute of Geophysics.

CHAPTER II - THE FORMATION OF MAUNA ULU

Since May 24, 1969, Mauna Ulu erupted almost continuously over a five year period until July 23, 1974 when activity finally ceased. On May 24, 1969, lava fountains broke out along an east-northeast trending fissure through Aloi Crater to north of Alae Crater. The lava fountaining became localized between these two craters, over the area where Mauna Ulu eventually formed. (figure 2.1.0)

By the end of 1970, Alae and Aloi Craters were both filled with lava by underground lava tubes and crater overflow from Mauna Ulu. Lava was able to enter the sea by lava tubes in June 1969 and September 1970.

Small pit craters developed, coalescing to form an elongate trench on the eastern flank of the volcano. In April 1971, the trench and summit crater merged to form a deep depression. Lava continued to enter the sea until May 1971. By October, lava completely disappeared from Mauna Ulu.

Voluminous fumes continued to be emitted from Mauna Ulu but lava did not return until February 1972. Activity intensity varied until a stable lava lake finally formed. A secondary vent opened at Alae Crater where another basaltic shield was built. From February 1972 to April 1973 approximately $125 \times 10^6 \text{ m}^3$ of lava erupted in the Alae-Mauna Ulu area, building up the shield volcano and the island of Hawaii.

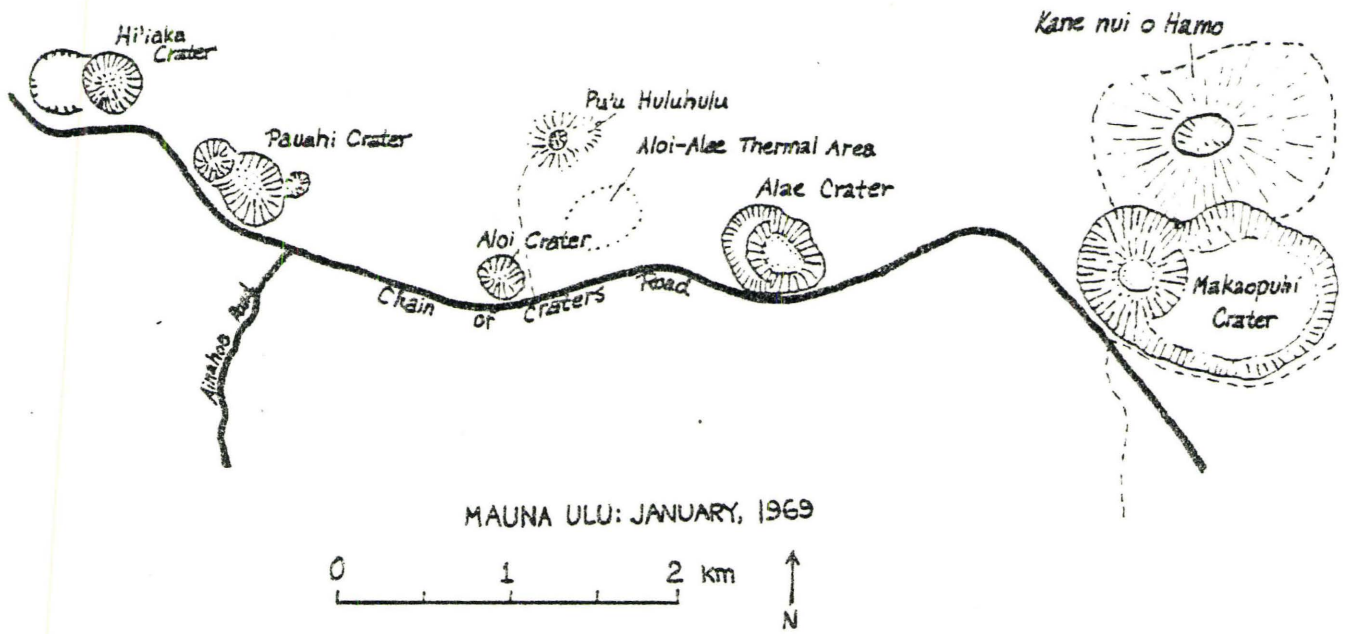
In April 1973, a 6.2 magnitude earthquake centered about 60 km north of Kilauea caused Mauna Ulu's lava lake to drain and the summit to deflate. Lava activity became concentrated uprift at Pauaki Crater and along the Koae fault zone;

Figure 2.1.0

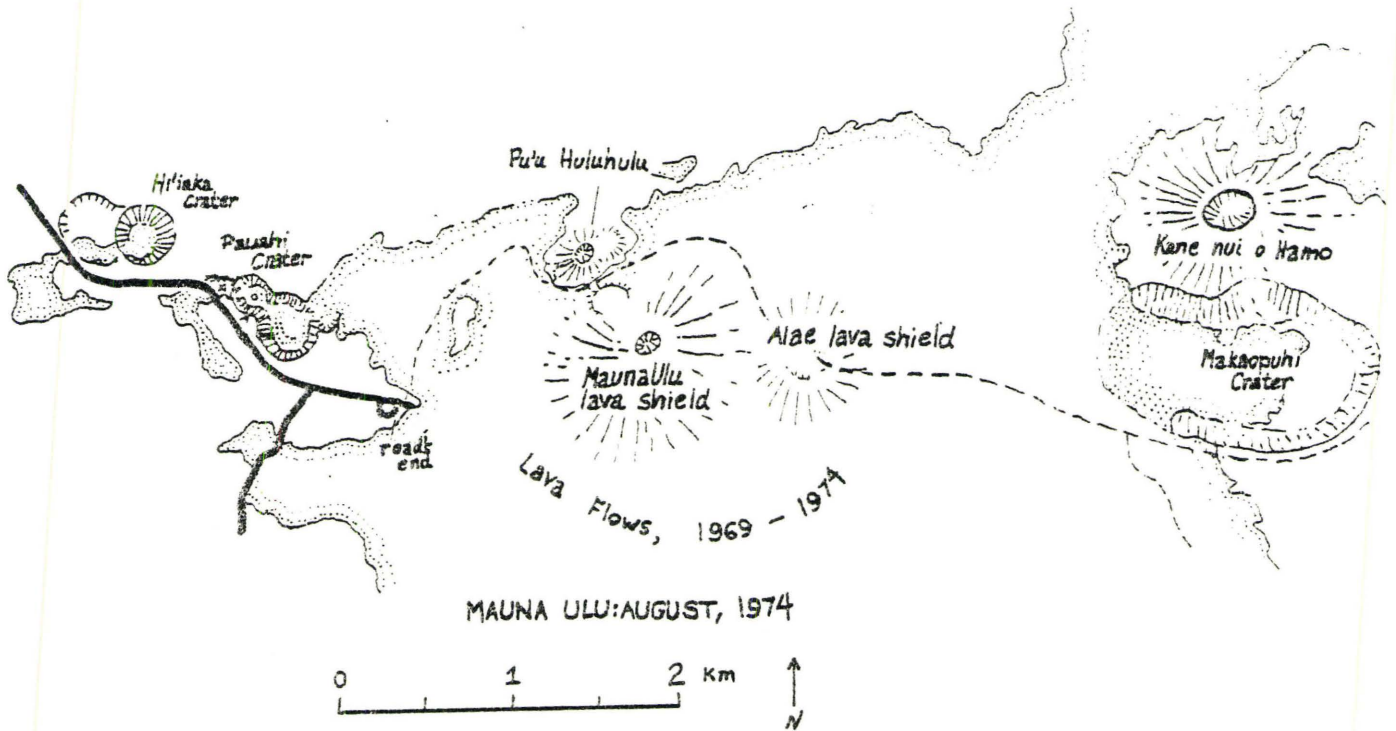
Aloi-Alae Thermal Area; area of
localized lava fountaining,
January 1969. (Hazlett, 1982)

Figure 2.2.0

Mauna Ulu Lava Shield; cessation of
activity, August 1974. (Hazlett, 1982)



MAUNA ULU: JANUARY, 1969



MAUNA ULU: AUGUST, 1974

for a short period of time. Lava never returned to Alae Crater though and Mauna Ulu remained fairly quiet.

In late September 1973, activity slowly started to increase at Mauna Ulu. Vigorous fountaining occurred but the overflowing lava lake suddenly drained on November 10. Within hours lava erupted near Pauaki Crater, but was halted by December.

At this time, activity resumed at Mauna Ulu. Eruptions were intense, with fountaining reaching up to 40 m. at times and overflows spreading over 9 km from the volcano. Activity intensified and weakened over a period of six months. The shield volcano grew about 30 m. in height and now stood 120 m. above the original flat lying area.

Activity quietened down by June and on July 19, seismographs reported the summit had deflated. The crater was empty of lava but still filled with fumes and vapours. Some lava fountaining occurred uprift at Kilauea's Caldera and isolated vents, but after July 23 lava never reappeared at Mauna Ulu. The long period of activity was over. (figure 2.2.0)

For the first time in 150 years, activity on Kilauea's flank had continued for more than a few weeks. Continuous observations were able to be made, allowing much improvement on the previous knowledge regarding volcanic processes. These processes include: lava fountaining, seismically controlled eruptions, volcanic shield growth, crater draining and filling, lava tube formation and volcanic island growth.

Hot gases and vapour have been issuing from vents on Mauna Ulu throughout its formation. Interaction of these gases with the lava on the volcano's now inactive summit, marked the initiation of the alteration process. Gas-rock interaction now became the dominant reaction process. Temperatures of the gases were likely much hotter at this time, with the volcano just starting to cool. As time passed, temperatures slowly decreased. The gases are now 100° - 250° C approximately; and it has been eight years since Mauna Ulu's eruptions were quietened.

It is surprising that with all the interest generated on Mauna Ulu, no one has studied the petrology of its summit region recently. The area is very colourful and certainly distinctive among the fields of grey and black lava which surround it. Actually, this is why the initial interest was generated for this thesis.

CHAPTER III - PETROGRAPHY

(3.1) Introduction

Approximately seventeen hand specimens were sampled from the thesis area. Sample 5 is ropy pahoehoe taken from the base of the shield volcano. All other samples were taken from the summit of Mauna Ulu; each specimen in varying stages of alteration. Table 3.1.1 outlines each hand sample and its distinguishing characteristics.

Fresh basalt in the Mauna Ulu area consists of both ropy pahoehoe and clinkery aa. The summit of the volcano has been depressed into a rock-filled crater. It is now about 120 m wide, 150 m long and 135 m deep (figure 3.1.1). Steam issues from vents, both in the walls of the crater (figure 3.1.2) and on the surrounding summit surface. Around the crater, across the top of the volcano, an alteration and decomposition of the basaltic structure has occurred. Little or no alteration is found within the crater where vent activity is at a minimum. Extensive alteration has pervaded the lava's structure elsewhere on the summit, where vent activity is at its maximum. A distinctive separation can be seen between altered and fresh lava on the upper flanks of the volcano. This boundary also marks the degree of vent activity; as it is at its lowest at the base of the volcano and within the crater.

A vent which emits only vapour and gases may be termed a fumarole. It is the most common means of venting air, steam

TABLE 3.1.1 Distinguishing Characteristics of Hand Samples

Sample	Vesicular framework	shiny, glassy appearance	coatings	inclusions	hard	crumbly	heavy (in weight)	light (in weight)	overall colour
1	x			light green	x			x	red-brown
2	x				amorphous material	x		x	orange
3	x				x	powder		x	orange-brown
4	x			light green	interior	exterior	x		light orange
5	x	x	white	light green	x			x	grey-black
6-1	x				framework	surface		x	light brown
6-2	x				framework	surface	x		light brown
7	x	x	white	white, green & yellow	x	patches	intermediate		brown & black
8	x				x	surface		x	orange-red
9	x				framework & amorphous	surface		x	red-orange brown
10	x	x	brown & white		x			x	black
11	x	x	brown		x			x	brown
12	x		white		x			x	brown & white
13	x					x		x	yellow-brown
14	x					x		x	yellow-orange
15	x					x		x	yellow-orange
16	x		light yellow			x		x	orange-yellow
17	x	x	red-brown yellow-white		x			x	brown-black

(cont) TABLE 3.1.1 Distinguishing Characteristics of Hand Samples

Sample	Crystal shape i.e. blades	powders				amorphous material	geopetal structure	concretionary structure	growths	other	Increasing degree of alteration
		white	yellow	orange	brown						
1	x									fresh	6
2	blades	x	x	x	x	x	x	x	x	altered	12
3	within vesicles	x	x	x	x	x	x	x	globular	altered surface	9
4	x	x	x	x	x	x	x	x	x	altered	10
5										fresh	1
6-1		x		x	x	x		x		altered	13
6-2		x		x	x	x	x	x	in vesicles	altered	13
7		x	x	x	x	x		x		fresh	5
8		x		x	x	x		x	globular	altered	8
9	x	x	x	x	x	x	x	x	globular & elongate	altered	11
10										fresh with coating	2
11		x		x	x	x	x	x		fresh with abundant coating	4
12		x				x	x	x		altered	7
13		x	x	x	x	x	x	x	globular	altered	15
14		x	x	x	x	x		x	globular	altered	16
15		x	x	x	x	x	x	x	globular	altered	14
16		x	x	x	x	x		x		altered	17
17		x			x					fresh	3

Figure 3.1.1

Rock filled crater on Mauna Ulu. Left foreground is altered lava at edge of crater. Depth to floor is about 135 m.

Figure 3.1.2

Steam issuing from a vent on the inside wall of the crater.



and other gases from a cooling volcanic deposit, (or in this case; a temporarily inactive volcano). Fumaroles are usually surrounded by colourful encrustations, which may or may not be sublimate (a solid phase deposited directly from a gaseous phase without becoming a liquid).

When Mount St. Helens erupted in 1980, numerous fumaroles were found, both near the crater, in direct association with the main vent (rooted) and within some of the lava flows (non-rooted). The encrustations surrounding the fumaroles were colourful yellow, orange, red and white deposits. A distinct similarity can be seen to those deposits on Mauna Ulu.

The chemistry of fumaroles on volcanoes of Central America has been studied extensively by Stoiber and Rose (1974) over an eleven year period. From their studies and analyses they have determined a generalized sequence of mineral zonation in encrustations, which they propose may apply to all known volcanic fumaroles. Their results are shown in Table 3.1.2.

Fumarolic vents on Mauna Ulu are concentrated only on the summit of the volcano, yet are relatively dispersed across the entire summit. (figures 3.1.3, 3.1.4). This is in direct contrast to fumaroles in Central America and Mount St. Helens, which are scattered across the volcano and its lava flows.

(3.2) Petrographic Study

Four thin sections were cut from samples 1,2,3,4, which were not too crumbly (friable). Initially an epoxy was required to be injected into the rock slab to aid in the

stability of the rock's delicate structure. Principally, the sections show how the basaltic lava has reacted to the alteration process. All alteration products were not able to be represented in thin sections.

The framework is a reddish brown basaltic glass which is opaque and extremely vesicular. Most vesicles are not whole but have been damaged through the thin section - making process. Commonly the pieces from some of the broken vesicles are found within the remnant vesicles as angular shards. (figure 3.2.1)

Spherulites are a function of devitrification of the volcanic glass framework, and are common in the altered samples. They have a radial pattern, with extinction crosses. Small, acicular light crystals, (1 mm in length); possibly relict plagioclase; are common within these spherulites (figure 3.2.2).

Olivine crystals (0.5 - 3 mm in size) are abundant, although whole euhedral grains are absent. Most whole grains are anhedral but several are only partial with relict hexagonal olivine outlines (figure 3.2.3). Olivine seldom alters to iddingsite but more commonly to iron oxides, along cross-cutting fracture-veins (figure 3.2.4).

Alteration evidence is seen in each sample. A rimming of iron oxide (red in reflected light-hematite). The rimming develops into a banding or zoning, very similar to that seen in hand specimen ("concretionary texture" section 3.4). The banding commonly shows colloform-type textures at

TABLE 3.1.2

Generalized zoning pattern of encrustations
around volcanic fumaroles (Stoiber & Rose, 1974)

Zone	Character	Colour	Approx T (°C)	Major Minerals	Other Minerals
A	Sulfate	White	900-400	Thenardite	Langbeinite, Anthitalite
B	Oxide	Brown or Black	300	specular hematite, Shcherbinita, tenorite	Cu, Zn vanadates? magnetite, cassiterite
C	Halide	white	150-250	Halite, fluorite	sylvite, sal ammoniac, cryptohalite, hydrophylite
D	Sulfate	dull red or dull pink	100-200	anhydrite	chalcocyanite, anglesite, langbeinite, thenardite, anthitalite, other sulphates, earthy hematite
E	Halide	Yellow or orange	≠100	raistonite, chloraluminite, earthy hematite, cristobalite	lawrencite
F	Sulphur- Gypsum	Yellow or White	≠100	sulfur, gypsum, earthy hematite	halotrichite, ilsemannite, other hydrated sulphates

Figure 3.1.3

Altered lava on Mauna Ulu's summit. Note steam vents in background. Crater is to the left.

Figure 3.1.4

Altered lava on Mauna Ulu's summit. Note steam and colour of material. Crater is to the left.



Figure 3.2.1

Large vesicle contains angular shards of the basaltic glass. Note zoning lining interior edges of vesicles. Olivine crystal at left lies in a spherulitic glass matrix (sample 2) (160x)

Figure 3.2.2

Spherulites (sample 2) (250x)

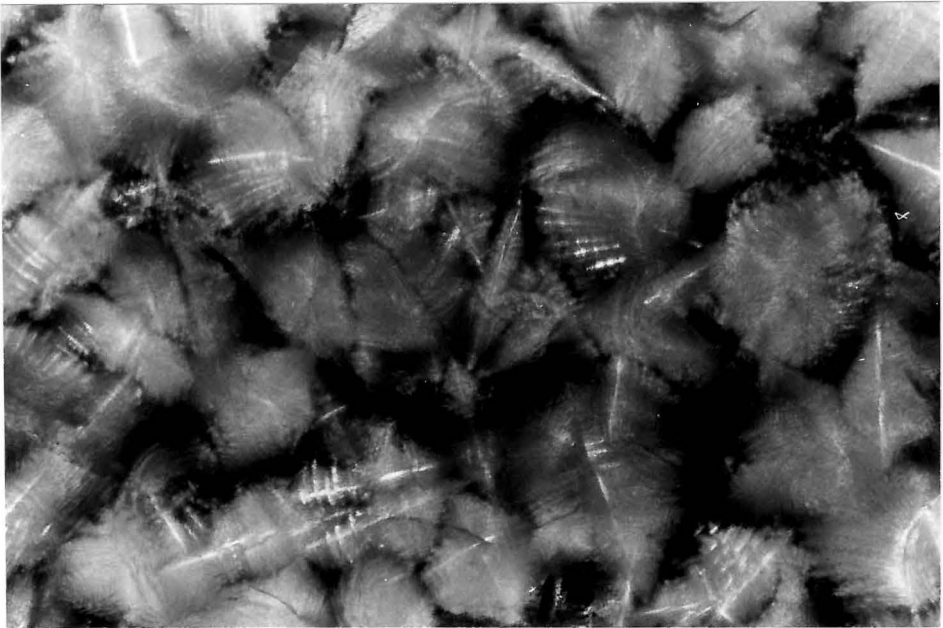
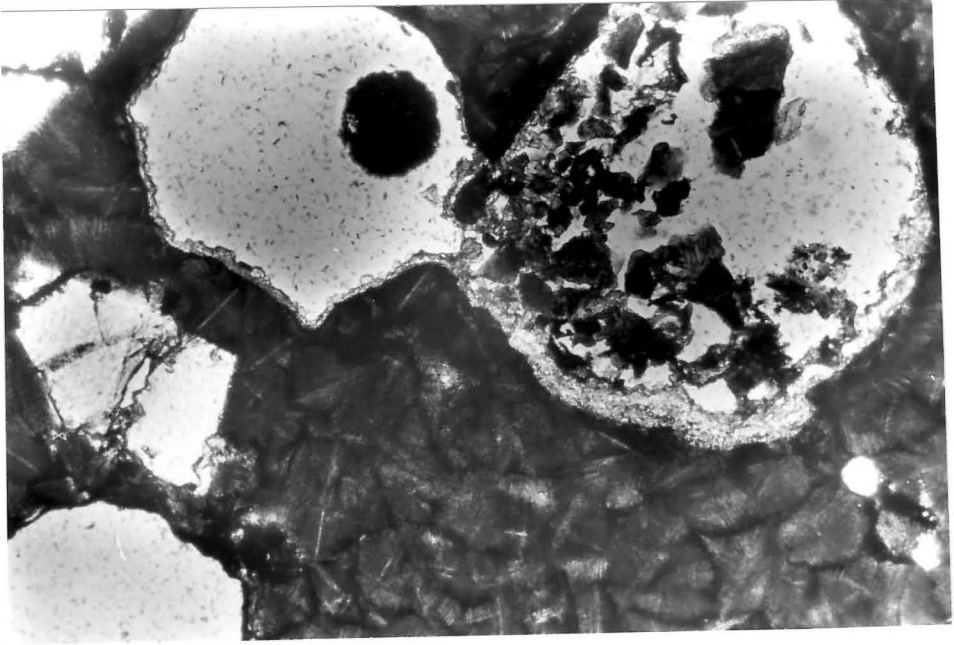
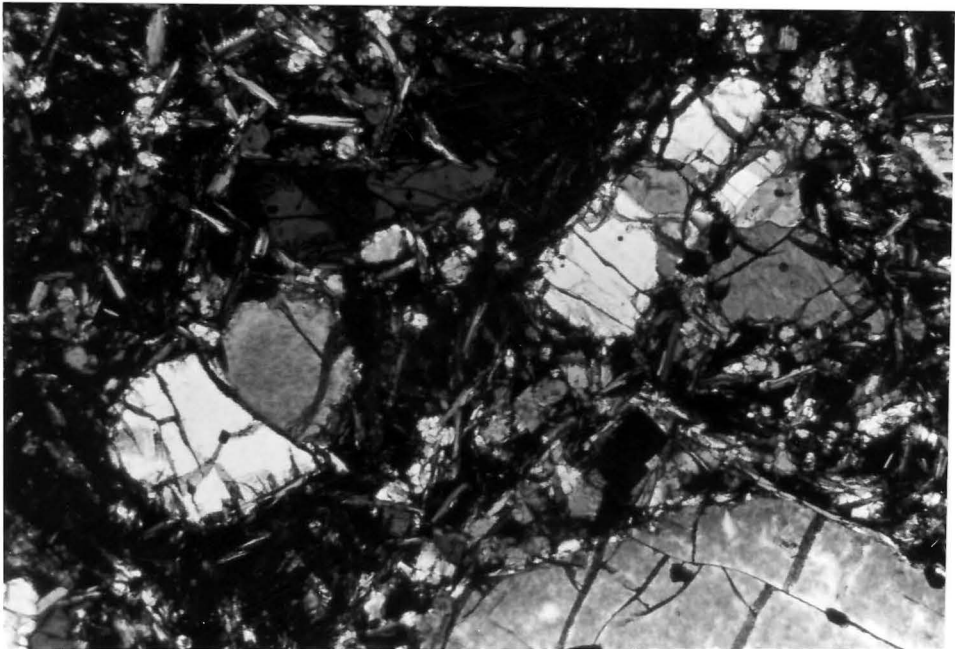
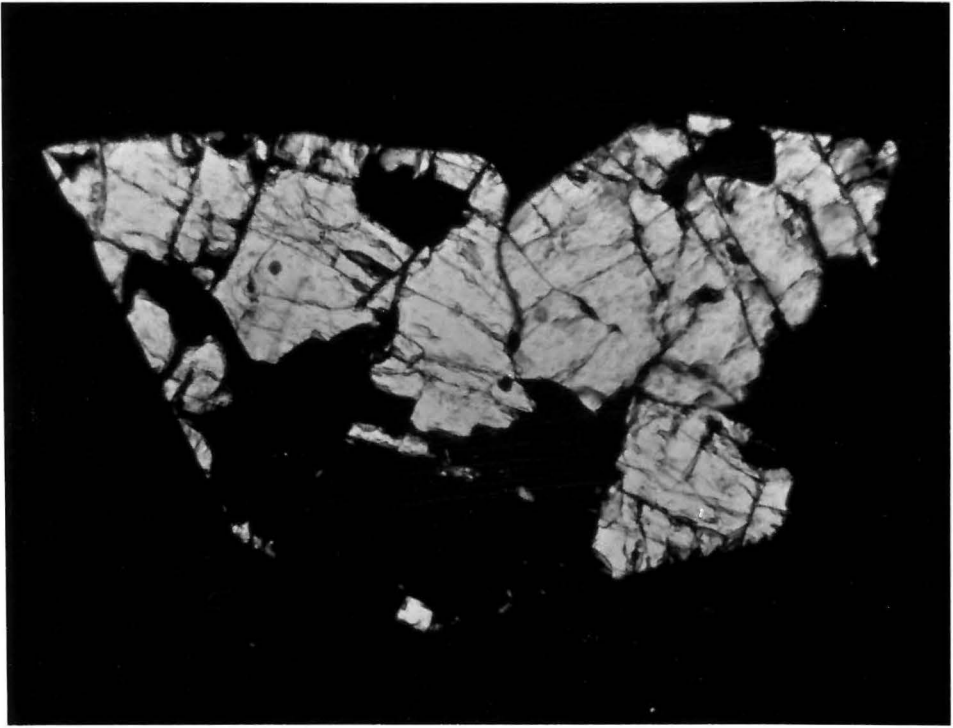


Figure 3.2.3

Partial olivine grains with relict crystal outlines (sample 1) (160x)

Figure 3.2.4

Altered olivine crystals in a plagioclase-rich matrix. Alteration products are iddingsite and commonly iron oxides. (sample 4) (63x)



the edges of, and within large vesicles (figure 3.2.5). It is pale brown to light orange in plain light; isotropic or radial with a "salt and pepper" texture in polarized light. The banding is likely opal and/or chalcedony, which are replacing both feldspar and olivine crystals from the matrix.

Sample four is interesting in that its exterior consists of altered material, yet its interior (when cut open) is fairly fresh, grey basaltic lava with olivine phenocrysts. (figure 3.2.6) This thin section shows a dense matrix of abundant Na-rich plagioclase feldspar (andesine) with minute olivine and possibly pyroxene grains. (figure 3.2.7). Lamellar iddingsite and red-brown iron oxides are also common with olivine in the matrix. Larger (0.5-3 mm in size) inclusions of anhedral, altered olivine also occur. (figure 3.2.4).

(3.3) Refractive Index Determination

From each hand sample, using a binocular microscope, isolated mineral and powder samples were hand picked from the whole rock. Five representative bulk rock samples were also hand crushed to a fine powder for use with XRF and for refractive index determination. Each sample was then studied under a petrographic microscope with respect to oils with varying refractive indices. Relative relations between indices of the sample and of the oil led to determination of the refractive index for the sample.

Poor results were obtained due mainly to the composition of the material. Most samples were glassy and amorphous, thus

Figure 3.2.5

Pale orange to light brown, colloformal-type banding between vesicles (sample 2) (63x)

Figure 3.2.6

Cut sample showing interior of fairly fresh basalt, and exterior of coloured alteration material. Note growths on surface and infilling of vesicles (near base). (sample four, top direction to upper left corner, base to lower right corner). (sample is 5.5 cm from top to bottom)

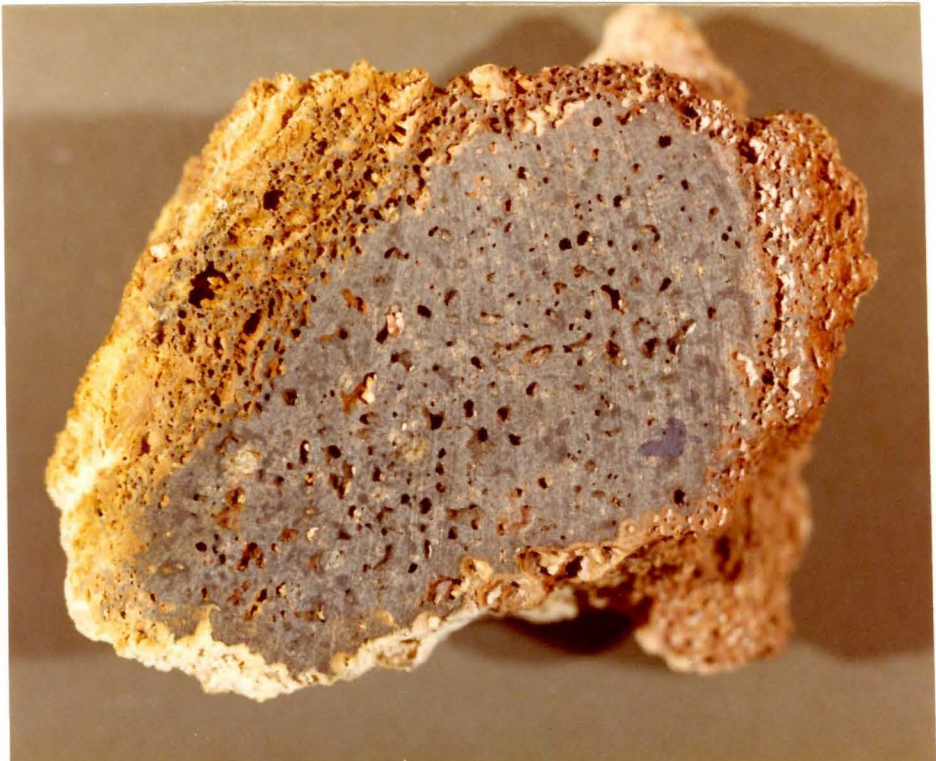
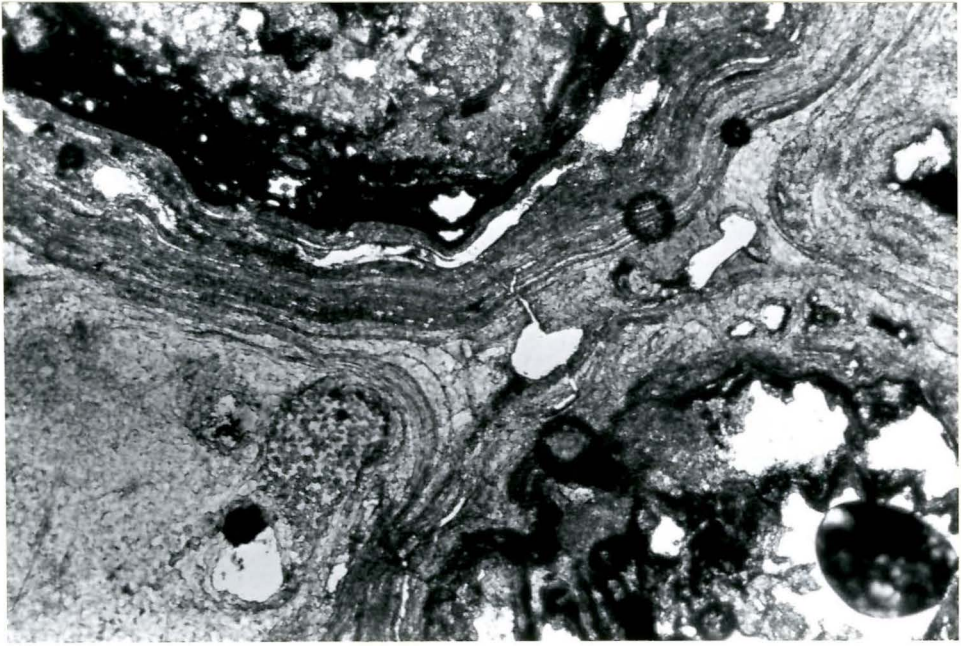
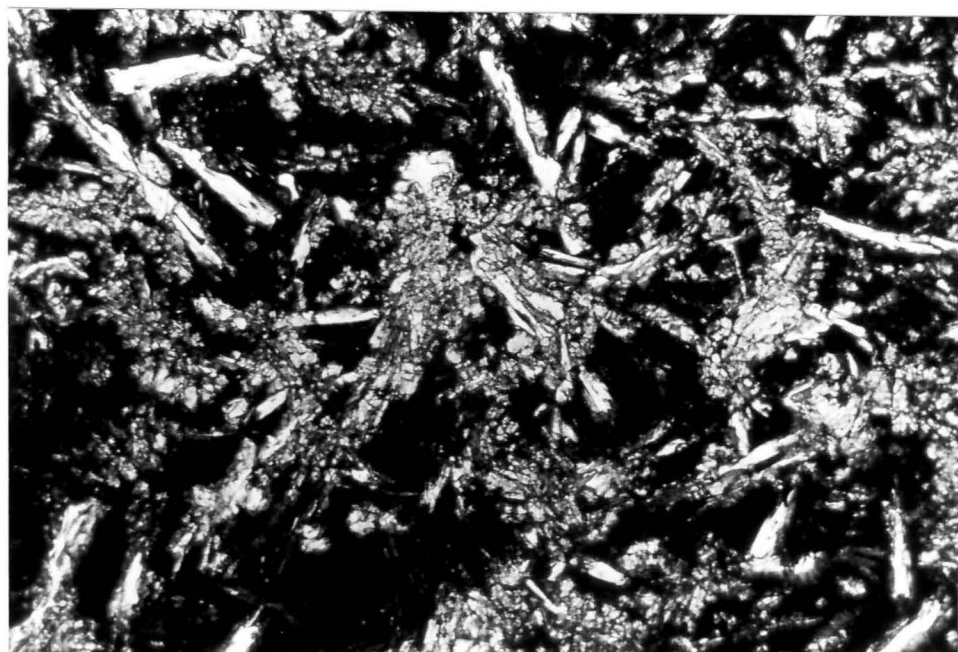


Figure 3.2.7

Dense matrix of Na-rich plagioclase laths
with fine grained olivine and pyroxene.
(sample 4) (250x)



show no crystal structure. All other materials indicated very fine grains with poor crystal shape; making crystallographic directions (α, β, γ) impossible to determine. The rare grains with good crystal shape which were obtained, were too infrequent to be able to use this method.

Data was not obtained for any hand picked samples, but crushed bulk rock samples one and five, enabled some results to be determined. Both samples are fresh lavas; five is grey-black pahoehoe and one is reddish-brown, hard vesicular basalt. Sample five contains minerals with refractive index of 1.660-1.664. Possible mineral species may be enstatite (α , 1.650-1.665; γ , 1.658-1.674), diopside (α , 1.650-1.698), or olivine (α , 1.651-1.681). Sample one contains minerals of refractive index 1.670-1.672. Possible minerals may be enstatite (γ , 1.658-1.674), diopside (α , 1.650-1.698), olivine (α , 1.651-1.681 and forsterite (γ , 1.670-1.680). (see Table 3.3.1) All possible minerals are either olivine or pyroxenes, but refractive indices are too high to include feldspars (i.e. andesine, 1.515-1.530).

It is interesting to note that before alteration, these minerals were large enough and distinct enough to be identified with refractive oils, yet, after alteration, no species with crystal structure is large enough nor well enough formed to be identified by their refractive indices.

Obviously, the alteration has degraded the mineral's crystal structure; and ultimately destroys it completely, leaving only an amorphous mass.

TABLE 3.3.1

Minerals with similar refractive indices as Samples
1 and 5

<u>Sample 1 (1.670-1.672)</u>		<u>Sample 5 (1.660-1.664)</u>		
(γ)	Anthophyllite	1.623-1.676	(γ) Prochlorite	1.599-1.667
(γ)	Hornblende	1.633-1.701	(α) Hornblende	1.614-1.675
(α)	Allanite	1.64 -1.77	(γ) Chondrite	1.621-1.670
* (α)	Diopside	1.650-1.698	(γ) Anthophyllite	1.623-1.676
* (α)	Olivine	1.651-1.681	(γ) Hornblende	1.633-1.701
(w)	Tourmaline	1.652-1.698	(γ) Glaucophane	1.639-1.668
* (γ)	Enstatite	1.658-1.674	(α) Allanite	1.640-1.770
(α)	Dumortierite	1.659-1.678	(γ) Prehnite	1.645-1.665
(γ)	Allanite	1.66 -1.80	* (α) Enstatite	1.650-1.665
(γ)	Cummingtonite	1.664-1.686	* (α) Diopside	1.650-1.698
(γ)	Jadeite	1.667-1.688	(α) Spodumene	1.551-1.668
* (γ)	Forsterite	1.670-1.680	* (α) Olivine	1.651-1.681
(α)	Lamprobalite	1.670-1.692	(w) Tourmaline	1.652-1.698
			(α) Jadeite	1.655-1.666
			(γ) Monticellite	1.655-1.669
			(α) Sillimanite	1.657-1.661
			(α) Grunerite	1.657-1.663
			* (γ) Enstatite	1.658-1.674
			(α) Dumortierite	1.659-1.678
			(γ) Allanite	1.660-1.800

*Possible mineral occurrences in olivine tholeiitic basalt

(3.4) Alteration Development

The change from fresh lava to an extensively decomposed material, begins with a film of non-crystalline material coating the surfaces and vesicles of the lava. This coating can be either white or a light reddish-brown colour. It forms or is deposited in paths of irregular shapes and sizes (figure 3.4.1). In some cases (figure 3.4.2), the coating is found in little rivulets along the surfaces of pahoehoe ropes. The surface appears to break down eroding away the tops of the vesicles and forming small ridges of more resistant lava, in the direction of lava flow (sample 11). Some of the vesicles which are coated, form a thicker coating which is wet-looking, and amorphous. It is very hard and is usually white or light orange in colour (figure 3.4.3).

Often a vesicle is "filled" from the bottom up with the amorphous material (spirit level), enabling top direction to be determined (figure 3.4.4). Fresh lava vesicles are barren of this type of texture; partially altered vesicles tend to alter from the base up. Extensively altered vesicles are almost totally filled with altered material. The interpretation arises that the amorphous material was precipitated from a gas as a sublimate, into the bowls developed by the lower portions of the vesicles. When sample 9 was broken open, interior vesicles showed the same type of texture as those on its exterior. (figure 3.4.5). The process must therefore permeate the porous basalt structure. Precipitation from a gas is a very plausible possibility for the formation of the amorphous material.

Figure 3.4.1

Coating of white and brown material on surface and within vesicles. (sample 12) (sample is 3 c.m. across)

Figure 3.4.2

Fresh ropey pahoehoe, with brown coating starting to fill in rivulets on surface. (sample 5) (sample is 3.5 cm from top to bottom).

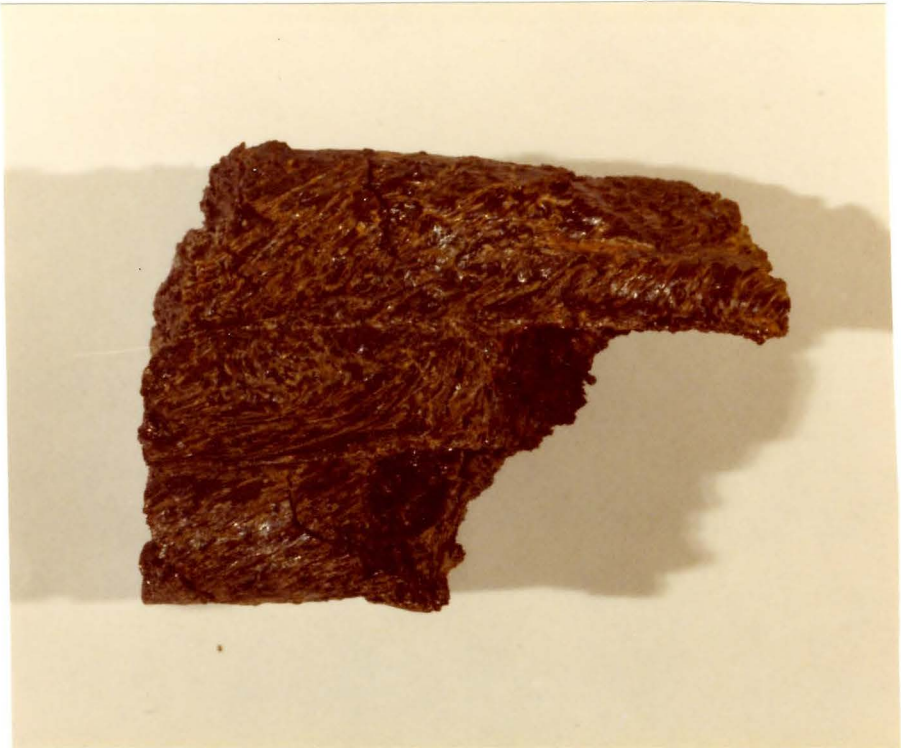


Figure 3.4.3

Underside of fairly fresh vesicular lava. Note coatings within vesicles and brown coating over surface. (sample 7) (sample is 5.5. cm from top to bottom)

Figure 3.4.4

Cut sample showing minute, vertical growths on upper surface and within vesicles; infilling of vesicles with amorphous material; concretionary texture. (especially in lower right section of the sample). (sample 2, surface at the top of the picture, base at the bottom). (sample is 4.5 cm from top to bottom).



In determining the composition of the amorphous substance, appearance, form, colour and hardness were all considered. It is also known that the solubility of SiO_2 in a water-rich hot gas is very high (GSA Memoir 97). The gas may tend to become super-saturated with SiO_2 , resulting in eventual precipitation as a sublimate; when temperatures are decreased.

"Concretionary structure" made up of layered or banded powdery crystalline material; forms in all altered samples. (figure 3.4.4). The basalt is altered from the exterior to the interior, in layers, as in an oxidation process. Every available surface is under attack, and becomes decomposed. In nearly fresh samples, basalt is thick between vesicles with little or no layering. In altered samples, the layering is thick, with only thin threads of basalt running between. The most decomposed samples are crumbly, consisting only of the layered material, without any basaltic framework.

The concretionary structure forms in the basalt around the vesicles; but within the vesicles, layers of amorphous silica are continually being built up. In extensively decomposed specimens, the concretionary structure and the amorphous layers merge to become indistinguishable from one another. (figure 3.4.5).

Light green olivine phenocrysts are common in fresh lava, but no evidence is seen of them in altered specimens. This is due either to their own decomposition and breakdown, thus they will not be identifiable after alteration; or, if the olivine is very resistant, the inclusions will become "coated"

Figure 3.4.5

Sample broken open to reveal its interior.
Note yellowish, orange, grey, slightly
shiny amorphous material. (sample 9)
(sample is 5 cm across)

Figure 3.4.6

Surface of sample showing white, orange
and yellow encrustations. Some globular
growths are visible. (sample 15) (sample
is 6 cm across)



and then hidden. In sample 9, there are several areas where the basalt has been broken to expose a "fresh" surface. A deep, forest green powder is located in these areas. The presumption is that this material is iron-magnesium rich (due to the colour) remnant forsteritic olivine, which has been chemically and structurally broken down. This suggestion is also reinforced by petrographic study (section 3.3). The green powder may thus be chloritic.

Colour is a prime factor in determining the stage of alteration that the rock has progressed to. In general, fresh samples are grey-black (figure 3.4.2), slightly altered samples are brownish (figures 3.4.1 and 3.4.3) more decomposed specimens turn orangey (figure 3.4.3) and those extensively altered samples have yellowish encrustations (figure 3.4.6) (Table 3.1.1). By observing which samples are fresh and those which are altered, and comparing the colours of powdery alteration products, one may conclude a pattern of colour change is associated with extent of decomposition. Samples 1, 5, 10 are fairly fresh and have no coloured "powders". Samples 12 and 17 have only brown or white powders. The more decomposed samples 6, 8, 11 have brown, white and orange coloured powders but no yellow. The most extensively altered samples 2, 3, 4, 7, 13, 14, 15, 16 have all four coloured powders forming their crumbly crusts. (figure 3.4.7).

To back up this pattern of colour change, one sees the entire sequence preserved in what are called "growths". These are minute, vertical extensions on the surface crusts and

Figure 3.4.7

Colourful surface of Mauna Ulu's altered deposits. Note variety of colours and crumbly texture.

Figure 3.4.8

Surface of sample, (note extensive oxidation as compared to Figure 3.4.7) showing botryoidal spheres. (sample 2) (sample is 8 cm across).



within some vesicles of many samples (figure 3.4.4). Whether all rocks originally had them but the growths were later destroyed is unknown, but the theory is suggested that these growths only formed in sheltered or protected local environments. Exposure to the elements may have discouraged growth formation in open areas.

The growths are circular, elongate extensions with globular tips. They "grow" vertically upward from the surface of the sample. They are about 1 mm in length by 0.50-0.75 mm in diameter. The growths seem sturdy; but they are made up of the same powder which makes up the rest of the crumbly crust, making them easily erodable.

Most growths have been partially broken, and not all growths show a continuous colour sequence, some colours being omitted; but a full coloured-powder trend can be determined. The base of the growths is brown to light brown, then zoned vertically upward, the colours change as follows: white, orange, yellow, white (sample 2) with various shades of these colours. It is noted that when a growth is "knocked off" a white powder underlies it. Many samples (3, 8, 9, 13, 14, 15) do not have fully developed growths on their surfaces. Instead, globular spheres, almost boitryoidal in appearance cover their altered surfaces (figure 3.4.8).

Sample nine consists of numerous concretionary patches of powder layered into coloured zones. The zoning is common but in some areas, a coloured layer may be wholly or partially removed. From the base, vertically upward,

Layering is as follows: white, reddish-orange, pinkish-white, red, with orange-yellow powder capping the sequence. Sample 2 shows a similar type of banding. The colours vary from reddish brown, light brown, pinkish white, yellowish white to white.

A polygonized fracture system was visible on the surface of one sample (8). Various colour zones could be seen across its smooth surface (possibly half of the interior of a large vesicle), but the surface has been cross-cut by very small, narrow vein-filled fractures. It appears that a vein consists of a powder of a couple shades darker than the colour of the powder which surrounds it. For example, red-brown patches are cut by brown veins; orange patches are cut by brown veins; yellow patches are cut by orange veins; and light yellow patches are cut by yellow veins. The veins or fractures usually form 120° angles with adjacent fractures. This polygonization may be due to a dessication or drying out process caused by a lack of damp hot gases.

The colour changes visible in hand sample may be due to temperature changes resulting from the cooling of the volcano, and cooling gases. Different gaseous temperatures will thus result in different alteration products, after reaction with the vent wallrock.

CHAPTER IV - GEOCHEMISTRY

(4.1) Introduction

Rock powders used for making the fused powder pellets were hand crushed with an agate mortar and pestle. Whole rock analyses were obtained using a Phillips Model 1450 AHP, sequential x-ray fluorescence spectrometer, within the Geology Department, McMaster University. A 6:1 flux (lithium tetraborate and lithium metaborate) to rock powder ratio was fused in platinum crucibles for 3-5 minutes at 1200°C for major element, whole rock analyses. All samples were analyzed by the author. In addition, one sample (14) was tested for its sulphur content. A value of 0.14% SO₂ was obtained using a Leco Corporation Sulphur Titrator, also within the McMaster Geology Department.

X-ray diffraction methods were attempted with several hand picked samples and crushed whole rock samples. The specimens are characterized by very high background levels without any dominant peaks obtained. This is indicative of amorphous substances within the altered deposits (Delthier, Pevear & Frank, 1980).

The data from the x-ray fluorescence work was analyzed by a McMaster University computer programme, which calculated and printed information such as: weight percents of oxides and CIPW norms, (Tables 4.1.1, 4.3.1). In order to compare the collected samples with fresh samples collected by other persons in and around Mauna Ulu, included are the

averages of 39 samples from Wright et al, 1975 in Table 4.1.1, for fresh tholeiitic basalt.

(4.2) Major Elements and Component Ratios

Figures 4.2.1, 4.2.2, 4.2.3, 4.2.4, 4.2.5 are graphical representations of changes in the weight percents of the oxides as alteration proceeds. Both SiO_2 and TiO_2 are increased in relative proportions to other oxides with increased alteration. Ti^{4+} is likely an impure minor component in the SiO_2 tetrahedron, with $\text{Ti}^{4+} \rightleftharpoons \text{Si}^{4+}$. It is assumed that any processes operating on the Si-O bonds in the tetrahedron will also react with the Ti-O bonds.

Figure 4.2.2 shows a large increase in Al_2O_3 and Fe_2O_3 in sample 9AA. This sample is rich in brown altered material compared to sample 9BB which is rich in amorphous material.

Note in sample 9BB the large sudden increase in weight percent SiO_2 , as compared to the slight decrease in sample 9AA. The increase of Al_2O_3 indicates that it must also be incorporated into sample 9AA. Note that Al_2O_3 decreases considerably in sample 9BB but Fe_2O_3 is only slightly decreased, indicating the inclusion of Fe-oxides with the amorphous opaline silica. MgO decreases in sample 9BB, and has about the same amount in samples 9AA and 13AA. Overall, increasing alteration shows a decrease in weight percent of these oxides.

TABLE 4.1.1 : X-Ray Fluorescence Results (normalized to 100):
Weight Percents of Oxides

	Without Prior Ignition						Ignited ² Prior to Analysis					
	(Wright) ¹											
	Mauna Ulu	1AA	5AA	9AA	13AA	14AA	1AA	5AA	9BB	13AA	14AA	
SiO ₂	49.37	48.47	49.22	46.19	71.29	88.65	49.24	49.30	70.96	71.34	88.16	
Al ₂ O ₃	12.56	11.63	12.03	20.08	7.02	1.98	12.01	11.94	6.97	7.18	2.19	
* Fe ₂ O ₃	11.61	13.23	13.23	19.44	9.91	2.15	13.92	13.33	12.96	9.94	2.14	
MgO	11.03	12.78	10.17	6.34	6.06	2.20	9.84	10.28	2.49	6.02	2.19	
CaO	10.19	9.15	10.26	4.00	1.53	0.67	9.57	10.37	2.60	1.63	0.70	
Na ₂ O	2.10	1.61	1.87	1.46	0.88	0.41	2.15	1.59	0.81	0.48	0.58	
K ₂ O	0.42	0.38	0.38	0.22	0.06	0.05	0.45	0.38	0.10	0.07	0.05	
TiO ₂	2.30	2.16	2.21	1.92	2.99	3.78	2.27	2.22	2.83	3.07	3.76	
MnO	0.18	0.21	0.22	0.13	0.04	0.03	0.17	0.20	0.07	0.03	0.02	
P ₂ O ₅	0.23	0.37	0.42	0.22	0.21	0.07	0.37	0.38	0.20	0.25	0.22	
*Total Iron							-0.42	-0.72	9.91	18.74	10.09	Loss on Ignition ³

1. Average of 39 samples of fresh tholeiitic Mauna Ulu Basalt (Wright et al, 1975)
2. Samples were ignited at high temperatures prior to x-ray analysis
3. Material lost due to ignition; omitted from sample normalization

Sample Descriptions

- 1AA - fresh red-brown basaltic lava
 5AA- fresh grey-black, pahoehoe lava
 9AA- iron oxide-rich material from sample 9
 9BB- amorphous-rich material from sample 9
 13AA- extensively altered lava
 14AA- extensively altered lava

Figure 4.2.1

Weight percent (SiO_2) vs sample
(M.U. is Wright's Maunu Ulu basalt).

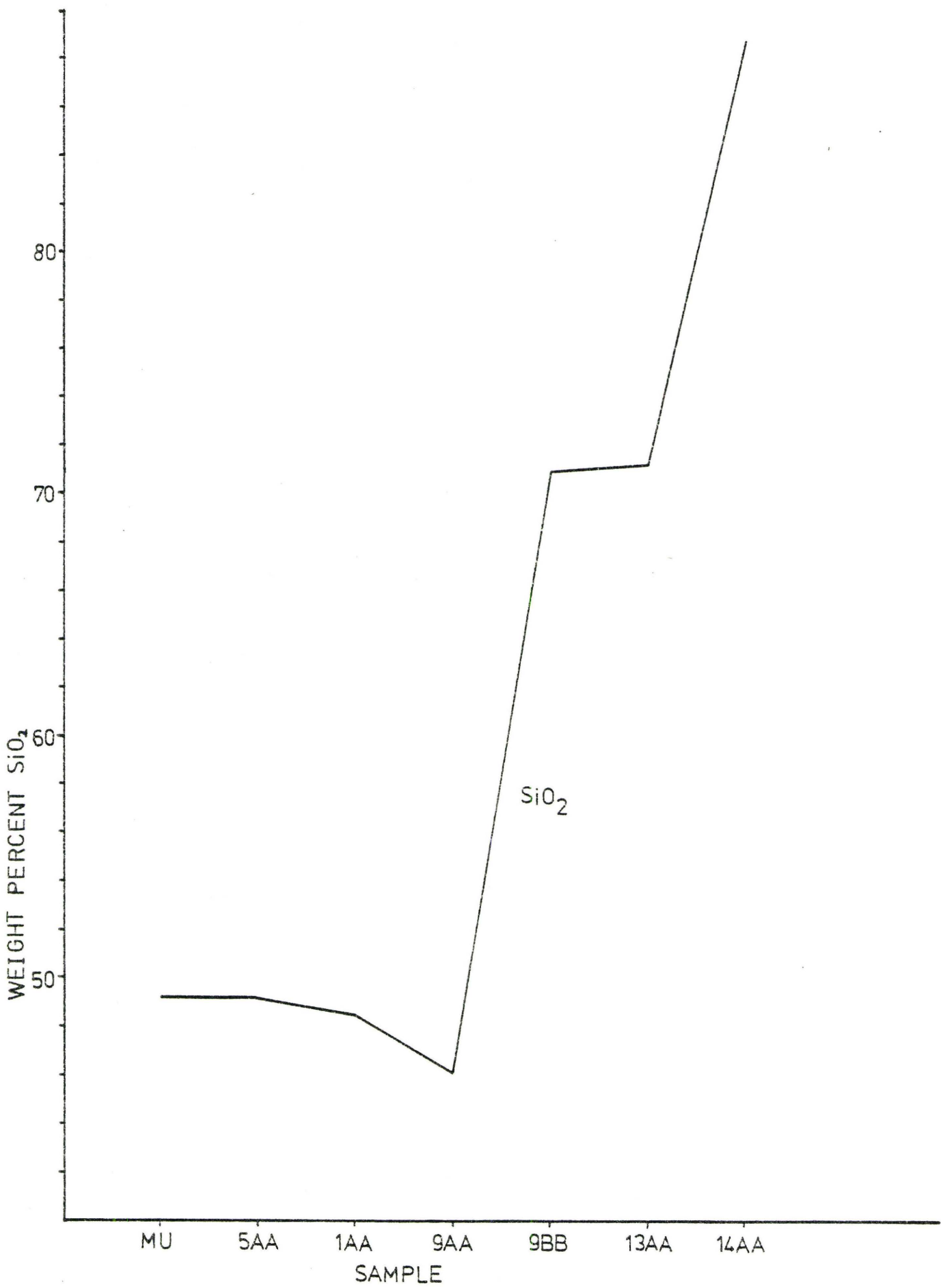


Figure 4.2.2

Weight percent (Al_2O_3 , Fe_2O_3) vs sample.

Figure 4.2.3

Weight percent (MgO , CaO) vs sample.

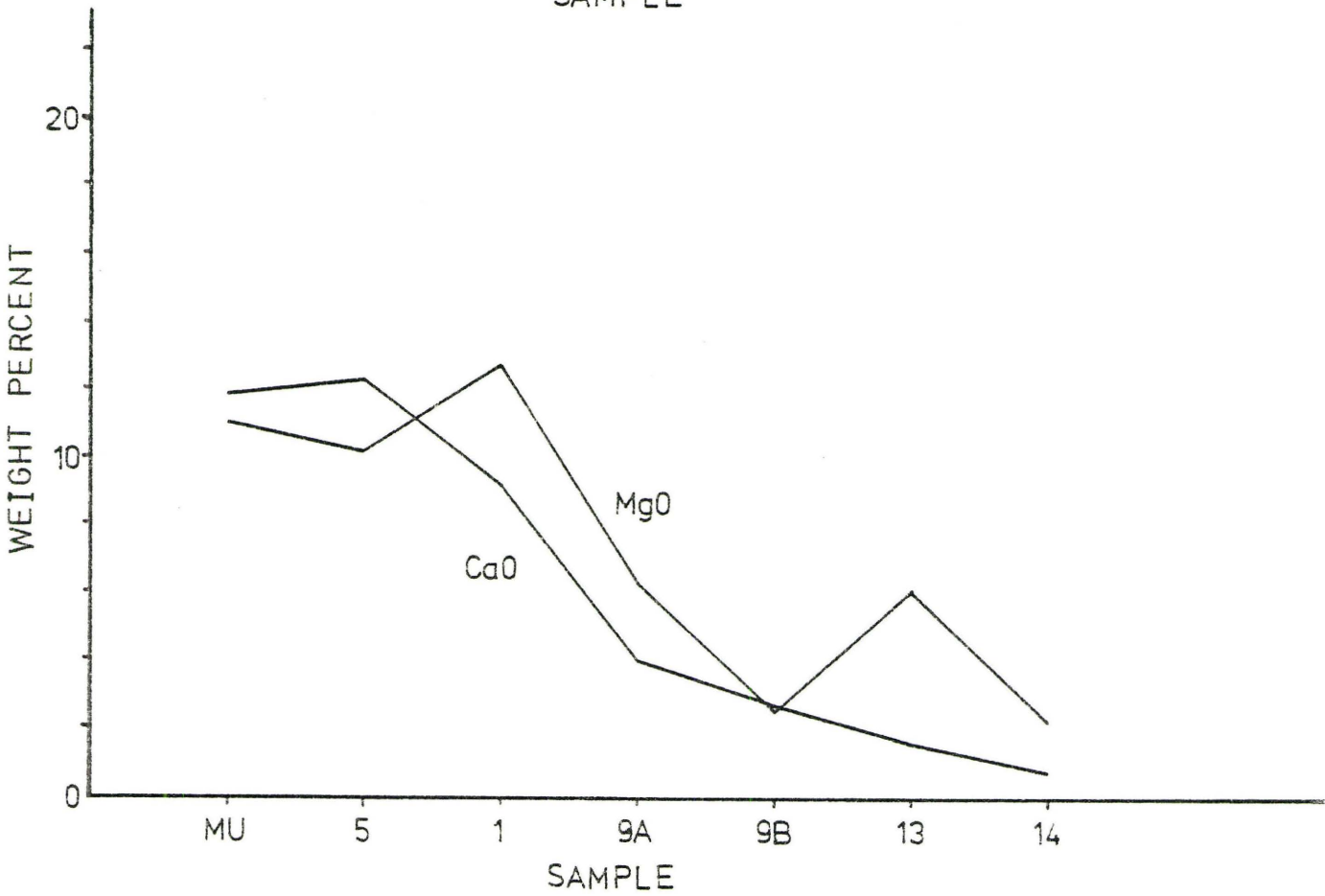
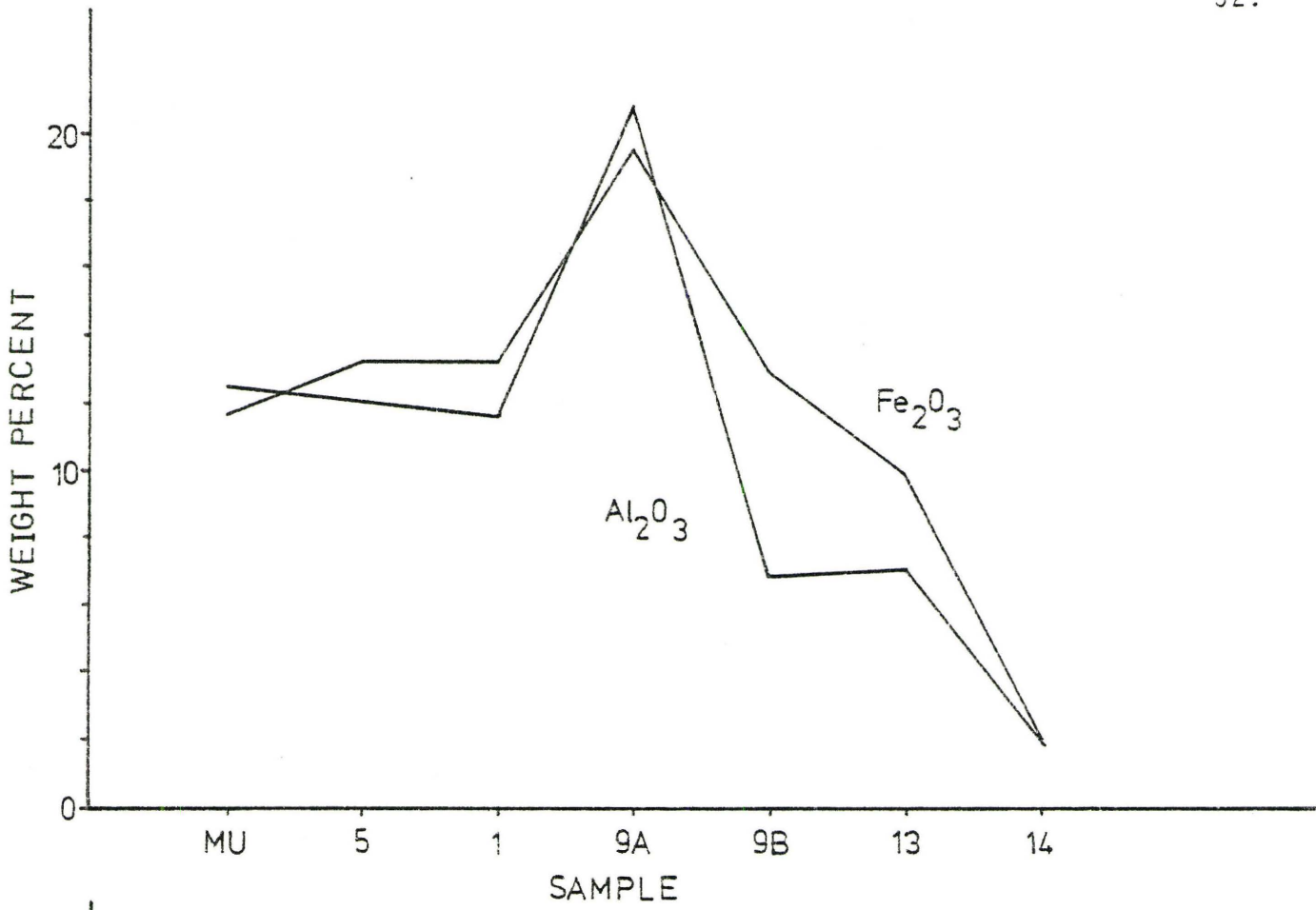
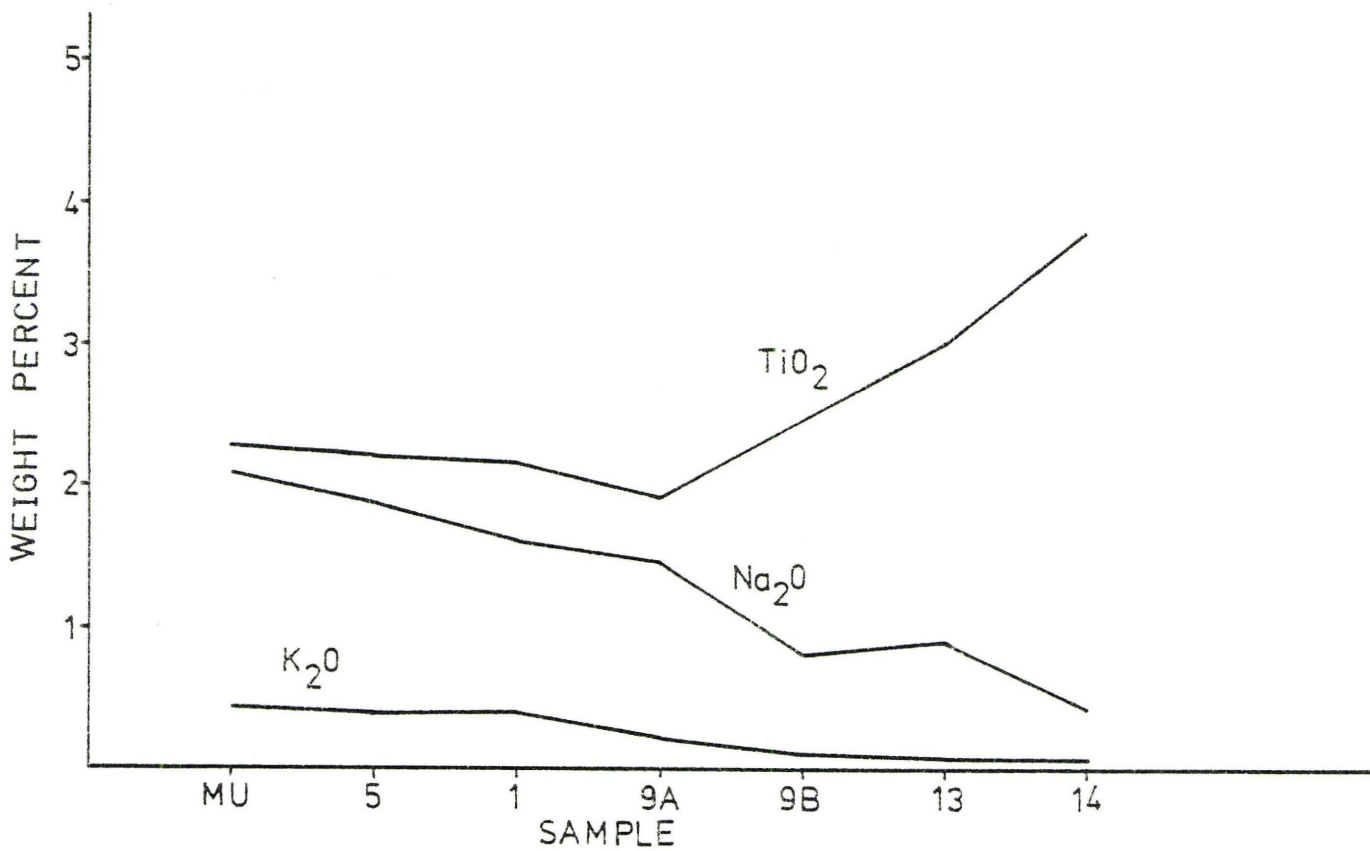
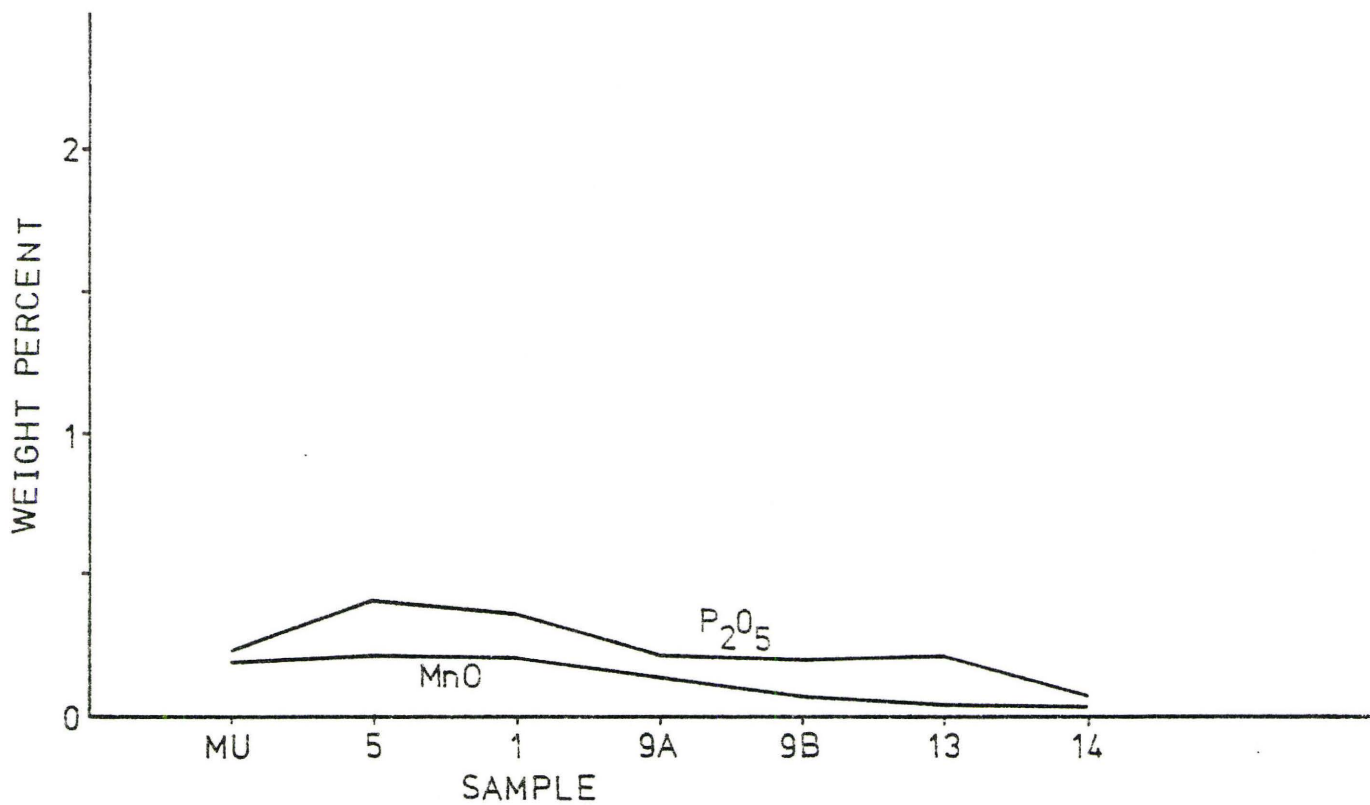


Figure 4.2.4

Weight percent (MnO , P_2O_5) vs sample.

Figure 4.2.5

Weight percent (TiO_2 , Na_2O , K_2O) vs sample.



The alteration appears to involve both a breakdown and an addition of material. The hard basaltic structure has been degraded to a crumbly powder, during the alteration process. At the same time, vesicles are being filled with dominantly amorphous material. From Graph 2.1, 2.5, SiO_2 and TiO_2 increase in relative proportion to the other oxides. The proposed process of alteration involves the breakdown of the hard framework (breaking of strong Si-O bonds) to a material which goes into a gaseous solution (hot gases are reacting with the lava) to be later deposited as an amorphous sublimate (no liquid phases are observed in hand samples or field studies) within the porous, crumbly, remnant lava structure.

Component ratios are shown in Table 4.2.1. From this data one can easily compare one oxide with proportions of several different oxides. Assume alteration trends proceed from left to right, from fresh to altered samples.

Two samples (9AA and 9BB) were taken from hand specimen nine. Sample 9AA is poor in amorphous material and comparatively richer in the red-brown iron oxides. Sample 9BB is rich in the amorphous substance. This information is reflected in the SiO_2 /oxide ratios; that for 9AA being very low, but that for 9BB is much higher (about the same as for sample 13AA, the next sample in the alteration pattern). The impression is that the amorphous substance is in fact silica, as the amorphous occurrences correlate with the occurrence of SiO_2 .

The alteration appears to involve both a breakdown and an addition of material. The hard basaltic structure has been degraded to a crumbly powder, during the alteration process. At the same time, vesicles are being filled with dominantly amorphous material. From Graph 2.1, 2.5, SiO_2 and TiO_2 increase in relative proportion to the other oxides. The proposed process of alteration involves the breakdown of the hard framework (breaking of strong Si-O bonds) to a material which goes into a gaseous solution (hot gases are reacting with the lava) to be later deposited as an amorphous sublimate (no liquid phases are observed in hand samples or field studies) within the porous, crumbly, remnant lava structure.

Component ratios are shown in Table 4.2.1. From this data one can easily compare one oxide with proportions of several different oxides. Assume alteration trends proceed from left to right, from fresh to altered samples.

Two samples (9AA and 9BB) were taken from hand specimen nine. Sample 9AA is poor in amorphous material and comparatively richer in the red-brown iron oxides. Sample 9BB is rich in the amorphous substance. This information is reflected in the SiO_2 /oxide ratios; that for 9AA being very low, but that for 9BB is much higher (about the same as for sample 13AA, the next sample in the alteration pattern). The impression is that the amorphous substance is in fact silica, as the amorphous occurrences correlate with the occurrence of SiO_2 .

$\text{SiO}_2/\text{Al}_2\text{O}_3$ ratio increases as alteration increases, except for 9AA which is low in SiO_2 and high in Al_2O_3 . $\text{SiO}_2/\text{Fe}_2\text{O}_3$ ratio increases except 9AA which again shows a low in SiO_2 and is high in Fe_2O_3 . SiO_2/MgO ratio increases gradationally except with 9BB which shows a sharp increase in SiO_2 as compared to MgO . $\text{MgO}/\text{Al}_2\text{O}_3$ and $\text{MgO}/\text{Fe}_2\text{O}_3$ ratios decrease except with 13AA and 14AA (very altered samples) which are low in Fe_2O_3 and Al_2O_3 . $\text{Fe}_2\text{O}_3/\text{Al}_2\text{O}_3$ ratio is fairly constant as alteration proceeds, except 9BB which is high in Fe_2O_3 . CaO/MgO decreases except 9BB which is low in MgO . $\text{CaO}/\text{K}_2\text{O}$ ratio is slightly decreased except for sample 5AA (fresh) which is high in CaO and K_2O (CaO K_2O) and samples 9AA and 14AA (altered) which are low in CaO and K_2O (CaO K_2O). $\text{Na}_2\text{O}/\text{CaO}$ ratio increases except 9BB which is low in Na_2O . TiO_2/MnO ratio increases and $\text{Na}_2\text{O}/\text{TiO}_2$, $\text{K}_2\text{O}/\text{TiO}_2$ ratios decrease as alteration proceeds.

In summary; fresh samples are high in K_2O , CaO , MgO , Na_2O , MnO , and relatively lower in SiO_2 and TiO_2 . Samples which have undergone alteration, become richer in SiO_2 , TiO_2 ; while K_2O , CaO , MgO , Na_2O , MnO abundances decrease. Fe_2O_3 (total iron) and Al_2O_3 show an initial increase with alteration but are subsequently then decreased in amount as alteration increases.

It may be interpreted that alteration proceeds stepwise, with continually changing chemistry (and mineralogy).

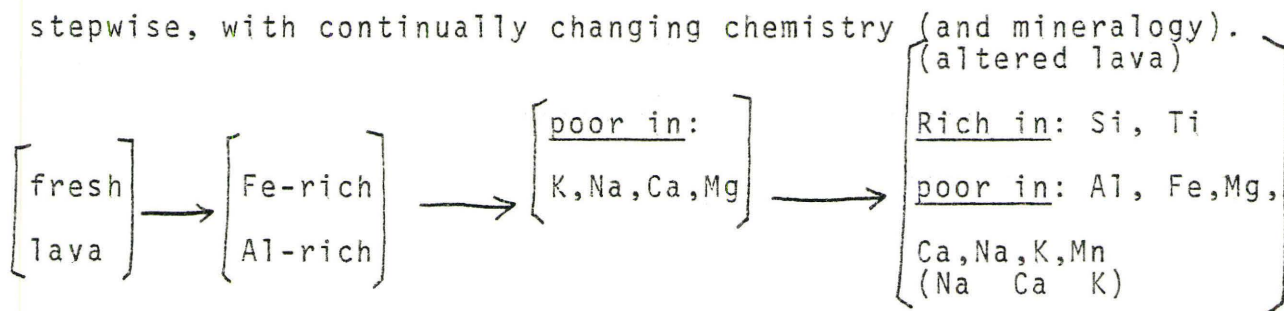


TABLE 4.2.1 COMPONENT RATIOS

	(Wright) Mauna Ulu ¹	1AA ²	5AA	9AA	9BB	13AA	14AA
$\text{SiO}_2/\text{Al}_2\text{O}_3$	3.93	4.17	4.09	2.30	10.18	10.16	44.77
$\text{SiO}_2/\text{Fe}_2\text{O}_3$	4.25	3.66	3.72	2.38	5.48	7.19	41.23
SiO_2/MgO	4.48	3.79	4.84	7.28	28.50	11.76	40.30
$\text{MgO}/\text{Fe}_2\text{O}_3$	0.95	0.97	0.77	0.33	0.19	0.61	1.02
$\text{MgO}/\text{Al}_2\text{O}_3$	0.88	1.10	0.84	0.32	0.36	0.86	1.11
$\text{Fe}_2\text{O}_3/\text{Al}_2\text{O}_3$	0.92	1.14	1.10	0.97	1.86	1.41	1.09
CaO/MgO	0.92	0.72	1.01	0.63	1.04	0.25	0.30
$\text{CaO}/\text{K}_2\text{O}$	24.26	24.08	26.76	18.18	26.00	25.50	13.40
$\text{Na}_2\text{O}/\text{CaO}$	0.21	0.18	0.18	0.37	0.31	0.58	0.61
$\text{Na}_2\text{O}/\text{K}_2\text{O}$	5.00	4.24	4.92	6.64	8.10	14.67	8.20
TiO_2/MnO	12.78	10.29	10.05	14.77	40.43	74.75	126.00
$\text{Na}_2\text{O}/\text{TiO}_2$	0.91	0.75	0.85	0.76	0.29	0.29	0.11
$\text{K}_2\text{O}/\text{TiO}_2$	0.18	0.18	0.17	0.11	0.04	0.02	0.01

1-see Table 4.1.1 for explanation

2-see Table 4.1.1 for sample descriptions

Keeping fresh lava as the standard, the steps of chemical changes upon alteration are shown above. This implies both gains and losses of these oxides but only in relative proportions to other elements (section 4.4).

(4.3) CIPW Norms

Weight percents of oxides were initially calculated with total iron as Fe_2O_3 . These were all re-calculated on a computer programme to obtain total iron as Fe_2O_3 and FeO ; as follows:

$$\% \text{Fe}_2\text{O}_3 = \% \text{TiO}_2 + 1.5 = 3.640$$

$$\% \text{FeO} = (\% \text{Fe}_2\text{O}_3 - \% \text{TiO}_2 - 1.5) \times 0.8998 = 8.521$$

It is assumed that TiO_2 is an occurring phase. Almost all samples had Fe_2O_3 FeO in amount. Sample 13 (altered) has slightly less FeO and sample 14 (altered) had FeO Fe_2O_3 ; so that the amount of FeO becomes negative in the computer programme. The programme was not designed for any type of alteration; thus, sample 14's data has been omitted. Normative calculations are listed in Table 4.3.1, with the understanding that these calculations are for unaltered rocks of the given compositions.

With reference to the normative calculations, there is little or no quartz (SiO_2) in fresh samples, yet it is abundant in altered samples. Orthoclase norm is high in fresh samples and decreases in altered ones. Albite (Na) and anorthite (Ca) show similar effects. All forms of diopside

TABLE 4.3.1: CIPW NORMS

	1AA	5AA	9AA	9BB	13AA
SiO ₂	48.945	49.699	46.928	71.571	71.664
Al ₂ O ₃	11.739	12.152	20.401	7.032	7.053
Fe ₂ O ₃	3.709	3.773	3.722	4.461	4.741
FeO	8.683	8.622	14.425	7.749	4.703
MgO	12.901	10.261	6.443	2.508	6.093
CaO	9.243	10.363	4.064	2.614	1.538
Na ₂ O	1.630	1.881	1.484	0.822	0.879
K ₂ O	0.377	0.380	0.224	0.107	0.058
TiO ₂	2.181	2.231	1.955	2.860	3.006
MnO	0.214	0.216	0.130	0.075	0.046
P ₂ O ₅	0.377	0.422	0.224	0.203	0.220
Qz ²	--	2.110	10.455	54.898	54.573
Or	2.228	2.246	1.324	0.632	0.343
Ab	13.793	15.917	12.557	6.956	7.438
An	23.602	23.594	18.700	11.643	6.194
Di(Wo)	8.264	10.465	--	--	--
Di(En)	5.811	7.062	--	--	--
Di(Fs)	1.750	2.607	--	--	--
Hyp(En)	26.090	18.492	16.045	6.246	15.174
Hyp(Fs)	7.858	6.826	20.427	5.961	--
Ol(Fo)	0.159	--	--	--	--
Ol(Fa)	0.053	--	--	--	--
Mt	5.378	5.470	5.397	6.468	6.595
Il	4.142	4.237	3.713	5.432	5.709
Ap	0.873	0.978	0.519	0.470	0.510
Cor	--	--	10.864	1.297	3.274
Hem	--	--	--	--	0.192

1-Sample 14AA is omitted due to type of computer programme used (see text)

2
 (quartz)
 (orthoclase)
 (albite)
 (anorthite)
 (Ca-pure diopside)
 (Mg-pure diopside)
 (Fe-pure diopside)
 (Mg-pure hypersthene)
 (Fe-pure Hypersthene)
 (Mg-pure olivine)
 (Fe-pure olivine)
 (magnetite)
 (ilmenite)
 (apatite)
 (corundum)
 (hematite)

(Ca, Mg or Fe-rich) may occur in fresh samples but are unlikely to form in altered samples, implying that these are poor in (Ca, Mg, Fe)-silicates; in diopsitic proportions. Hypersthene results imply that Mg-rich forms dominate in amount in all samples; except 9AA, which is high in Fe (therefore Fe-rich hypersthene dominates). Olivine is not expected to form in any altered samples. Magnetite, ilmenite and apatite are all calculated to occur in similar proportions in each sample.

Normative corundum seems likely to be found only in altered samples, due to the availability of free Al. The alteration has probably broken down alumino-silicate minerals, releasing free Al. This is indicated by the occurrence of corundum in the norm calculations. Hematite is only calculated to occur in sample 13AA which is altered. This may also be due to the fact that in previously altered sample, the Fe has been used in forming other compounds; and only in the most extensively altered samples does free Fe become available to react only with oxygen; to form hematite.

(4.1.4) Composition - Volume Relationships

A metasomatic alteration involves the introduction of material from an external source; and depending on the conditions, a corresponding amount may be lost from the system. Under some circumstances, metasomatism may result in the complete replacement of one mineral by another without loss of the original texture. Recrystallization may also occur if the fluids involved are energetic enough; to continue to react with the mineral species.

Figures 4.4.1, 4.4.2, 4.4.3, 4.4.4 indicate the actual amount of material lost or gained in the alteration process, assuming it was metasomatic. The method followed is from Gresens (1967). In a metasomatic replacement $aA + \downarrow(X)\uparrow \longrightarrow bB$, a , b are amounts (in grams) of each mineral (A,B); $X = x_1 + x_2 + \dots + x_n$, X is the total amount of material lost or gained (in g), x_n are the constituent components; C_n^z is the weight percent of component n in mineral z ; fv is the volume factor change (V_B/V_A); g_n is the specific gravity of mineral n . $x_1 = a \left[fv \left(\frac{g_B}{g_A} \right)^A c_1^B - c_1^A \right]$. It is convenient to assume $a = 100$ g, and $fv = 1$ (no volume change, although this is only the ideal case). The Mauna Ulu basalt composition determined by Wright (M.U.) is assumed to be the fresh basalt, and its density is assumed to be 2.772 g/cm^3 (Tilley, 1922).

Specific gravities of each crushed whole rock sample were found using a water displacement method (Hutchison, 1974) where specific gravity = mass/volume. (Tables 4.4.1 and 4.4.2; and Appendix A for sample calculation).

In the graphs the components which simultaneously cross the gain-loss zero line are immobile components in the reaction process. Those components which vary somewhat from the zero line are slightly mobile, and components which vary considerably from this gain-loss zero line are mobile components in the metasomatic process. From the graph, the mobile components are: SiO_2 , Al_2O_3 , Fe_2O_3 , MgO , CaO ; slightly mobile components are: TiO_2 , Na_2O , and immobile components are K_2O , MnO , P_2O_5 . (note scales).

Figure 4.4.1

Gain and Loss (grams) (SiO_2) vs sample
(very mobile)

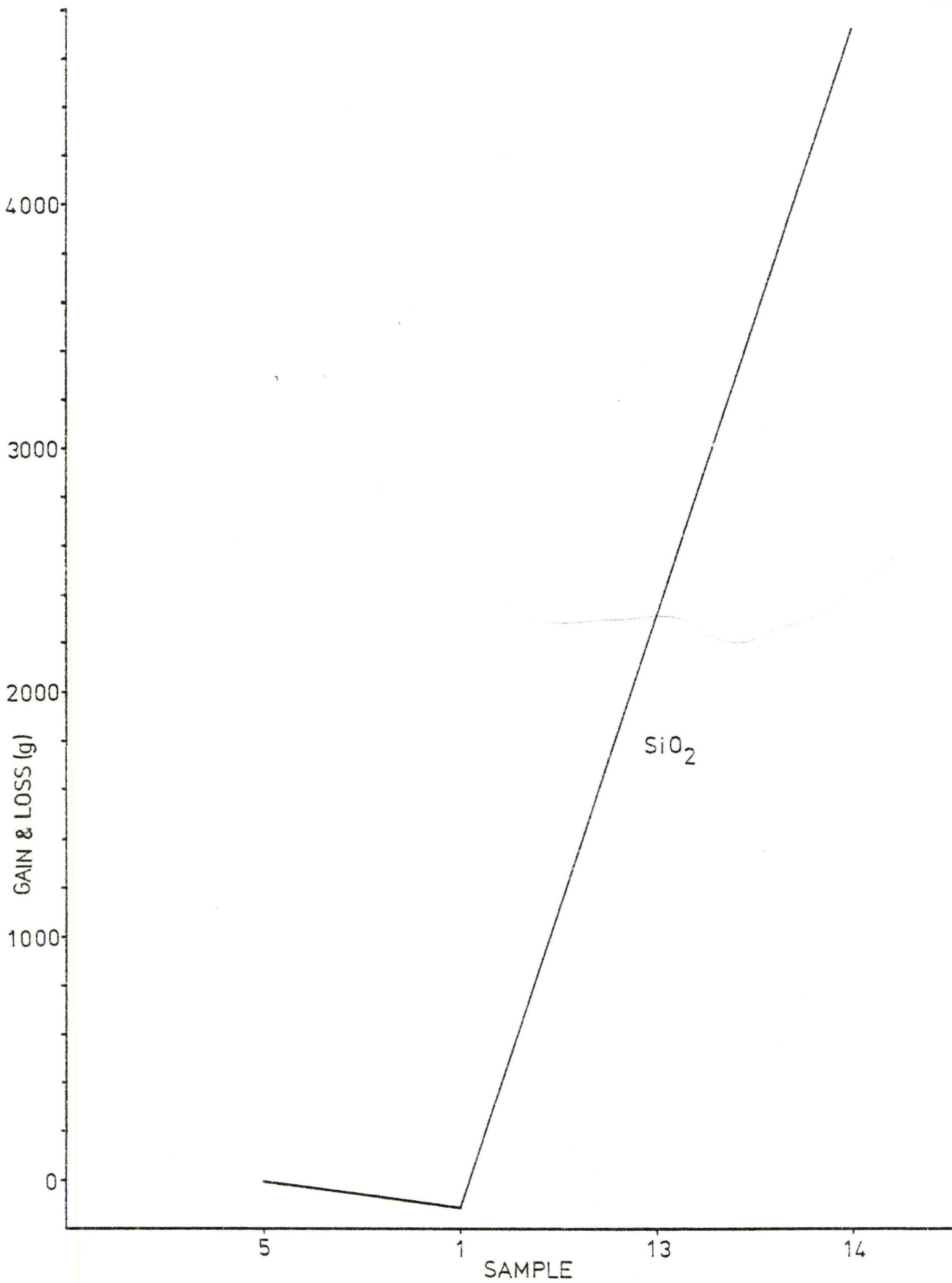


Figure 4.4.2

Gain and Loss (grams) (Al_2O_3 , Fe_2O_3 , MgO , CaO)
vs sample.

(mobile)

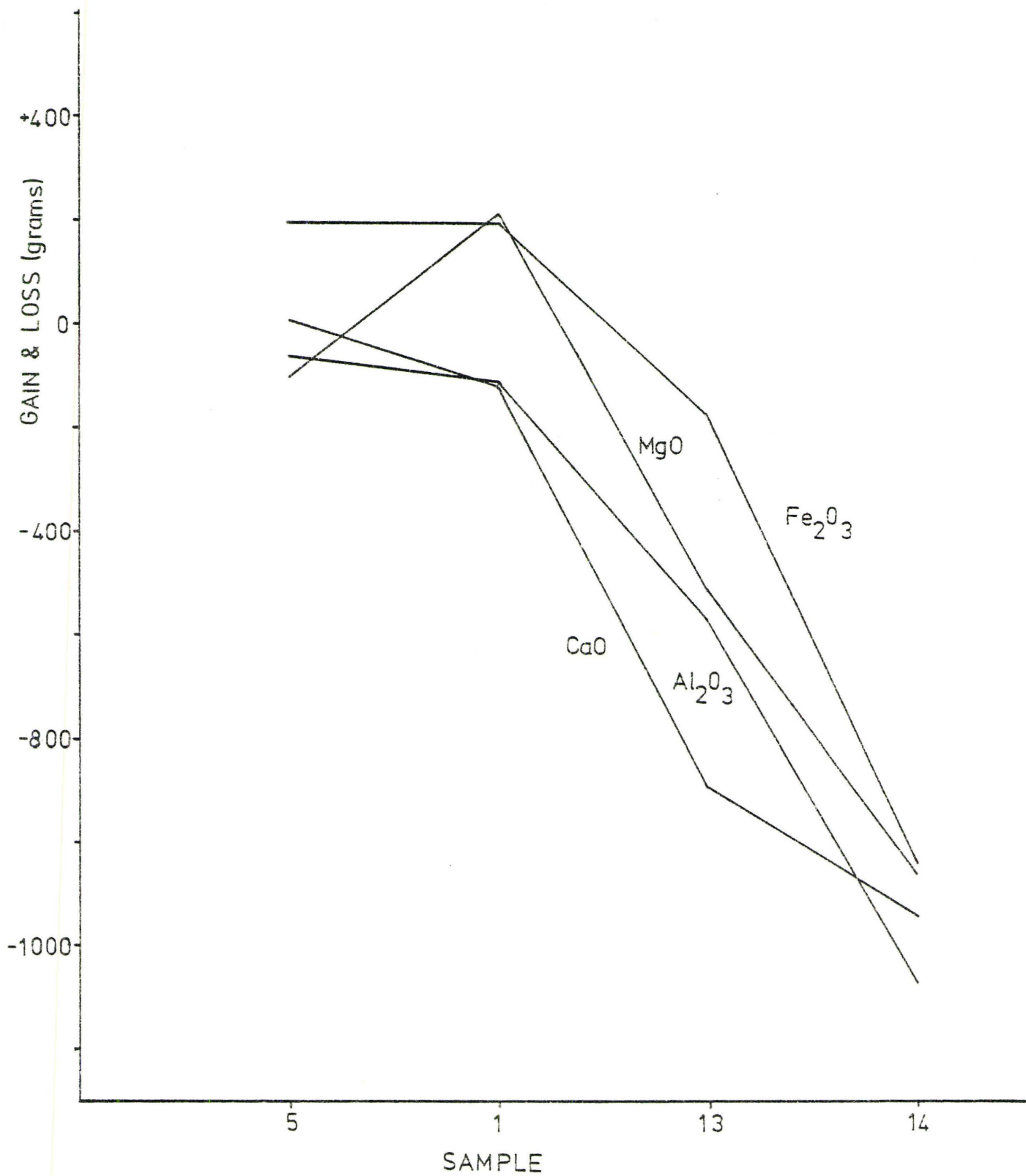


Figure 4.4.3

Gain and Loss (grams) (TiO_2 , Na_2O) vs sample.
(slightly mobile)

Figure 4.4.4

Gain and Loss (grams) (K_2O , MnO , P_2O_5) vs sample.
(immobile)

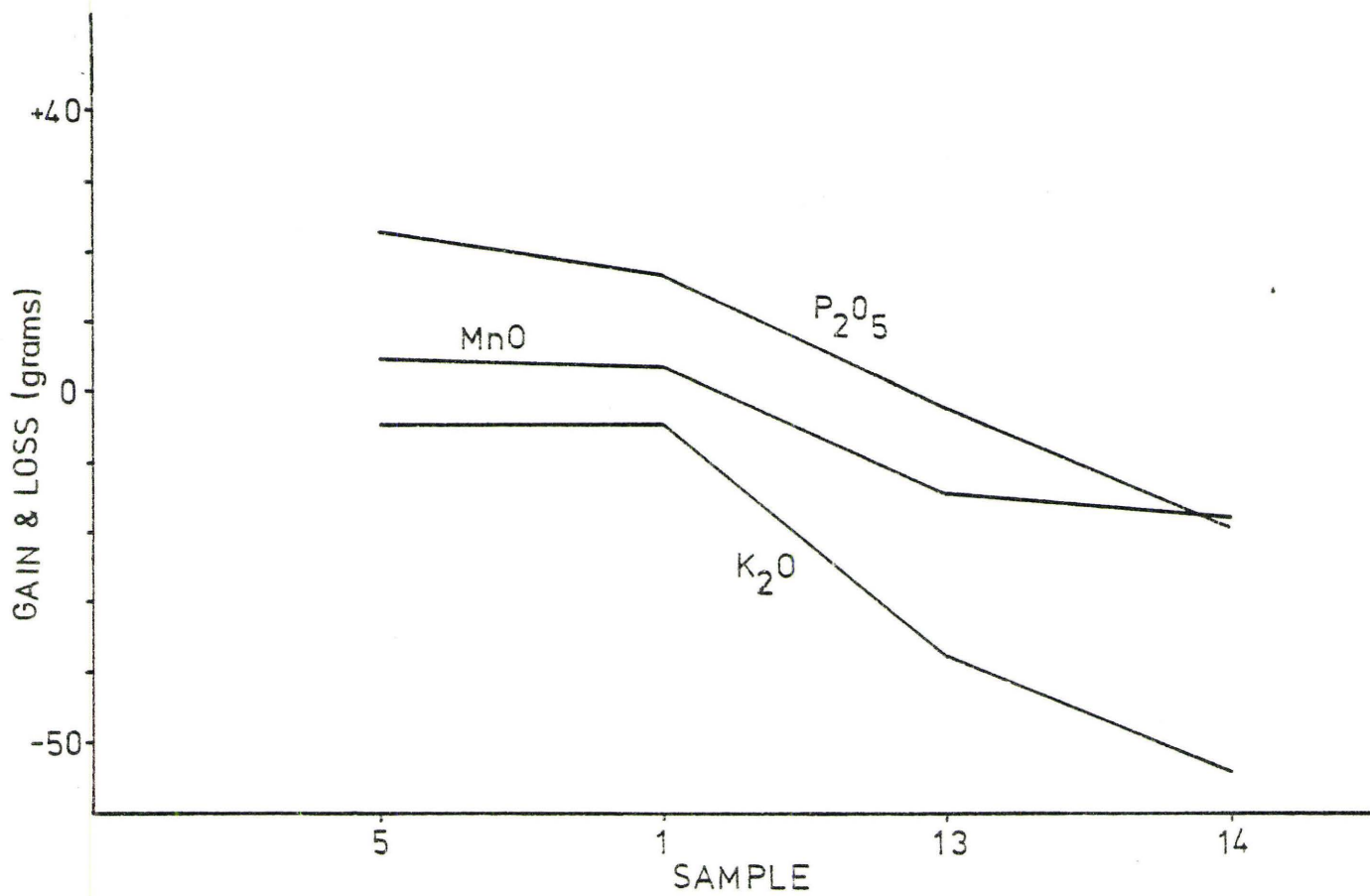
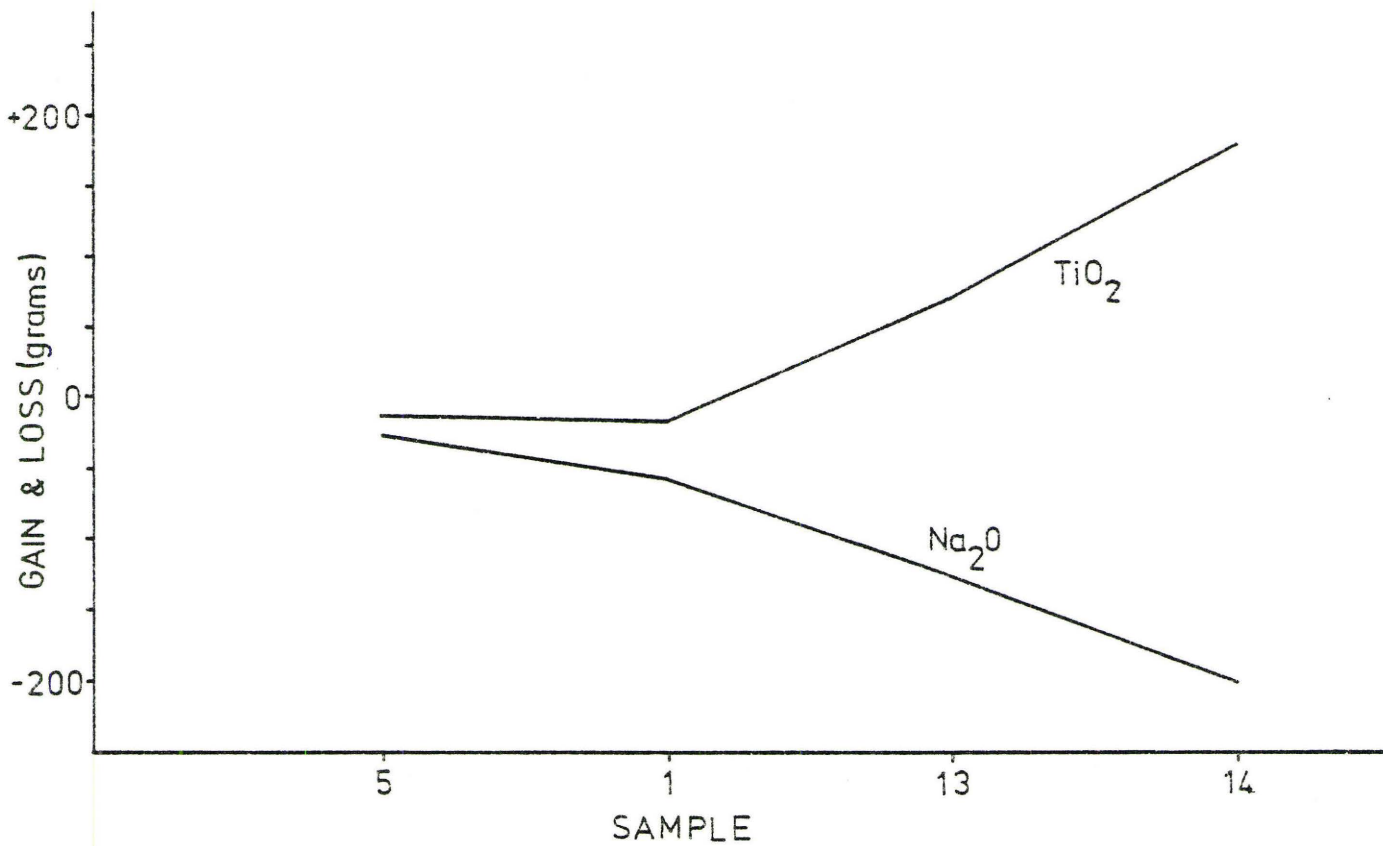


Table 4.4.1

Specific gravities of samples used for gain-loss determination (determined by displacement method, Hutchison, 1974)

Sample	Specific gravity (g/cm ³)
fresh basalt	2.772 (Tilley, 1922)
5AA	3.330
1AA	3.330
13AA	2.860
14AA	3.330

Table 4.4.2 Absolute Gains and Losses (grams)

fresh basalt (Wright's M.U.¹) + 1(x)↓ → (sample shown below)

x_i	5AA	1AA	13AA	14AA
x_{SiO_2}	-18.02	-108.12	2261.59	4718.70
$x_{Al_2O_3}$	-63.67	-111.72	-571.59	-1270.97
$x_{Fe_2O_3}$	194.61	194.61	-175.40	-1136.43
x_{MgO}	-103.31	210.23	-512.78	-1060.75
x_{CaO}	8.41	-124.94	-893.49	-1143.64
x_{Na_2O}	-27.63	-58.86	-125.87	-203.02
x_{K_2O}	-4.81	-4.81	-37.14	-44.45
x_{TiO_2}	-10.82	-16.82	71.19	177.79
x_{MnO}	4.81	3.60	-14.44	-18.02
$x_{P_2O_5}$	22.82	16.82	-2.06	-19.22

1-See Table 4.1.1 for explanation

This implies that K_2O , MnO , P_2O_5 play no part as reactants in the alteration process, yet all other components do so in varying degrees. The most reactive is obviously SiO_2 , seen by the large increase on Graph 4.2.1.

Relating the variances in amounts to the mineralogy of the samples, one concludes the following. Al is likely found in the plagioclase feldspar structure, with Ca and Na cations. Mg and Fe are cations in the olivine and pyroxene structure. Si is ubiquitous in the structure of all feldspars, pyroxenes and olivines, thus it is the most likely to react under the proper conditions. (i.e. source of Si is not a problem).

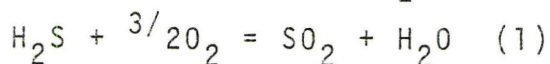
When these minerals are chemically and physically broken down, the cations (including Si and Al) are free to react with any available phases. The gain-loss results are thus possible evidence of mineral destruction and alteration.

CHAPTER V - VOLCANIC GAS COMPOSITIONS

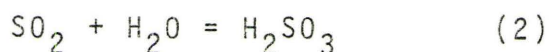
In understanding the nature of fumarolic alteration deposits it is necessary to have a knowledge of the volcanic gases emanating from the fumaroles. The composition of the gas relays much information about a volcano, the evolution of its magma and the resultant lava composition.

The gas compositions from basaltic volcanoes are all approximately similar, excluding minor regional variances. The chemistry of gases emanating from Mount St. Helens has been studied by Casadevall and Greenland (1980). They sampled from both low and high temperature fumaroles with the following results: 96% of the gas at low temperature fumaroles ($<150^{\circ}\text{C}$) was air (including H_2O), with minor amounts of CO_2 , CO , SO_2 , H_2S , CH_4 . (CH_4 content is about the same as in air). 68-85% air (including H_2O) was found at high temperature fumaroles (828°C) with minor CO_2 , CO , CH_4 , SO_2 , H_2S , COS , in the gas.

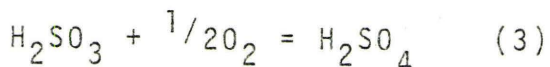
H_2S is the dominant sulphur gas at high temperatures, and SO_2 is dominant at low temperatures. They suggest that sulphur is released from the melt as H_2S but is rapidly oxidized.



SO_2 will become oxidized by reaction with steam, ground water etc., to form sulphurous acid droplets. (or aerosols).



These droplets may become oxidized by the atmosphere to form sulphuric acid.

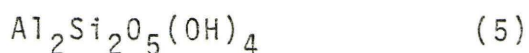
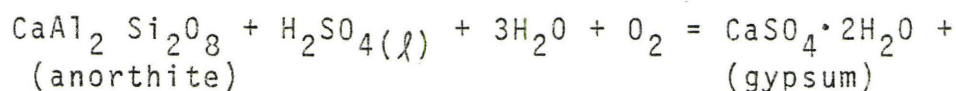
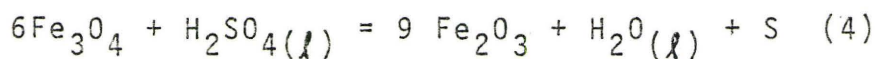


They believe that these reactions lead to the formation of abundant sulphates, which are common around fumaroles on

Mount St. Helens.

Stoiber and Rose (1974)(section 3.1) considered volcanic gas equilibria in their extensive studies of Central American volcanoes. They noted that high temperature gases are emitted at the fumarole opening. Direct field measurements indicate that as distance from the opening increases, the gases become cooled and P_{O_2} is increased. Under certain conditions changing temperatures and oxygen partial pressures will thus enable material to be deposited as a sublimate, from the fumarolic gases.

They also found that H_2S and H_2SO_4 gases dominate over SO_2 gas at high temperature ($800^{\circ}K$) fumaroles for a total pressure of 1 atm and a range of P_{O_2} . At $500^{\circ}K$, SO_2 gases dominate over H_2S gases for a range of P_{O_2} . They noted that at temperatures below $608^{\circ}K$ (boiling point of H_2SO_4), sulphuric acid liquid aerosols in the gas will form; (even more likely below $500^{\circ}K$) and tend to coat the wallrock, resulting in an acid alteration. As temperature decreases, the aerosols will become dilute enough to dissolve other gaseous components. These reactions may be represented as follows: ($150^{\circ}C$).



(dickite, kaolinite or halloysite)

These reactions are the effects of reaction of sulphuric acid with the wallrock. Halogen acid alteration of the wallrock may result in the formation of chloraluminat

($\text{AlCl}_3 \cdot 6\text{H}_2\text{O}$) and ralstonite ($\text{NaMgAl}(\text{F},\text{OH}) \cdot \text{H}_2\text{O}$), which are common as fumarole encrustations. Stoiber and Rose concluded that the fumarolic gas consisted of H_2O , SO_2 , HCl , HF , CO_2 with minor volatile cations.

Naughton (1980) collected gas and condensate samples along the southeast rift of Kilauea volcano in 1977. The gas samples consisted mostly of air with CO_2 , H_2 and SO_2 , (and minor H_2S) gases also occurring. Condensate samples were characterized by high contents of fluoride and chloride in an acid medium (pH 2). Minor amounts of Na, Mg, K, Ca, Cu, also occurred.

Gerlach (1980) studied gas analyses from Kilauea Volcano also. His recent analyses contained N_2 , H_2O , O_2 ; CO_2 , H_2S and SO_2 . He also noted that H_2S was the dominant sulphur gas at higher temperatures, whereas SO_2 dominated at lower temperatures.

Naughton et al (1974) studied the chemistry of sublimates on Mauna Ulu (Table 5.1.1). The sublimates were collected in the fumes directly above the active lava fountain in the volcano's crater. Dilute sulphuric acid droplets were common, as was the deposition of opaline silica directly from the fumes. Persistent gases in the fume clouds were CO_2 , SO_2 , HCl and HF . It is believed that reactions (2) and (3) were occurring. Both reactions probably occur easily and are probably catalyzed by metallic ions in the fume cloud.

The sublimates contain a large proportion of SO_4^{2-} in addition to Na^+ , Ca^{2+} ; which is most likely the source for the formation of sulphates. Sulphates (Na_2SO_4 , CaSO_4) should thus be common constituents in the alteration deposits of Mauna Ulu.

TABLE 5.1.1

Chemistry of the sublimate collected above Mauna Ulu's lava fountain in January, 1970 (Naughton et al, 1974)

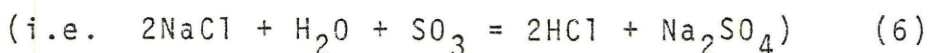
weight %, moisture excluded

<u>Major Cations</u>		<u>Minor Cations</u>		<u>Anions and other</u>	
Na	4.1	NH ₄ ⁺	0.22	SO ₄ ²⁻	74.0
K	1.5	Ti	0.33	Cl	5.4
Ca	3.5	Zn	0.25	F	1.6
Mg	2.2	H ⁺	0.22	B	0.59
Al	2.8	Cu	0.12	SiO ₂	0.39
Fe	2.6	Ni	0.04		

Hawaiian oceanic volcanoes do not usually contain very large amounts of Cl, F, B, NH_4^+ , yet these constituents have relatively larger proportions on Mauna Ulu. This is indicative of the formation of halides as alteration deposits.

Naughton et al detailed the vaporization process near a lava fountain into three steps: (1) vaporization from the lava of all species to form gases; (2) particulates "grow" as the gas becomes supersaturated and condenses; (3) cooling, further condensation and further reaction. Assume equilibrium for all steps.

Results of gas analyses are shown in Table 5.1.2 and figure 5.1.1, in terms of the three vaporization steps. Several items may be noted from this figure. Water and CO_2 are approximately constant as are Na_2SO_4 and CaSO_4 ; once they are formed. The most changes occur with SO_2 , SO_3 and H_2SO_4 over the range of conditions. Halides tend to dominate at higher temperatures whereas sulfates are dominate at lower temperatures, possibly due to reaction with H_2O and SO_3 .



For simplicity, several reactions were omitted from figure 5.1.1. From a reduced environment at 1400°K to an oxidized one at 400°K , the reactions are

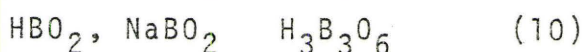
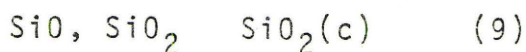
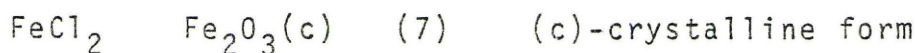


TABLE 5.1.2 Calculated equilibrium composition of major (controlling) gaseous components under various conditions of oxidation and temperature. (Naughton et al, 1974)

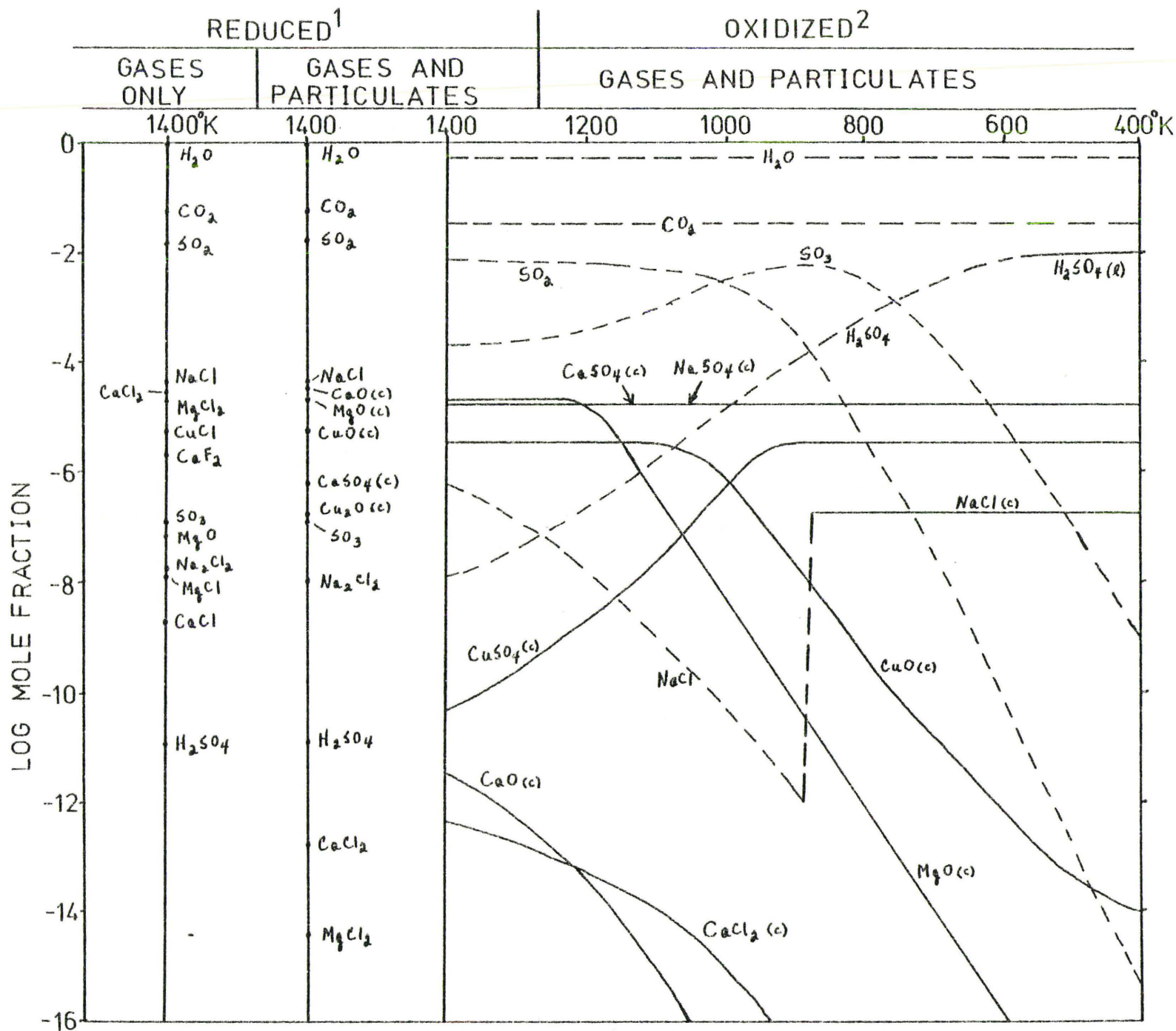
Mole Fractions			
	1400 ⁰ K Reduced ¹	1400 ⁰ K Oxidized ²	400 ⁰ K Oxidized ²
H ₂ O	0.95	0.63	0.63
H ₂	2.6×10^{-3}	2.1×10^{-8}	1.6×10^{-29}
O ₂	2.6×10^{-8}	0.070	0.067
CO ₂	0.040	0.027	0.027
CO	2.4×10^{-4}	2.2×10^{-10}	4.4×10^{-34}
SO	3.6×10^{-6}	1.4×10^{-18}	3.0×10^{-53}
SO ₂	0.010	6.4×10^{-3}	3.8×10^{-18}
SO ₃	1.2×10^{-7}	2.0×10^{-4}	7.8×10^{-11}
H ₂ SO ₄ ³	1.1×10^{-11}	1.3×10^{-8}	6.6×10^{-3}
HCl	2.8×10^{-4}	1.9×10^{-4}	1.1×10^{-4}
HF	1.7×10^{-4}	1.1×10^{-4}	9.6×10^{-5}
N ₂	1.8×10^{-5}	0.27	0.27

- 1- "Reduced" refers to a condition of equilibrium with Hawaiian lava at 1400⁰K (1127⁰C), with oxygen fugacity approximately equal to 10⁻⁸ atm. (Fudali, 1965).
2. "Oxidized" refers to a mixture with atmospheric oxygen with the oxygen content reduced to about 7 percent by the predominant water vapour from the fume.
3. H₂SO₄, liquid phase; condenses at 476⁰K

Figure 5.1.1

Calculated equilibrium compositions of compounds of the elements H, O, C, S, Cl, Na, Ca, Mg and Cu present above 10^{-16} mole fraction (Naughton et al, 1974)

- 1- Reduced refers to $pO_2 = 10^{-8}$
- 2- Oxidized refers to air which is assumed to be diluted about half (10% O_2) with the water vapour of the fume
- c- crystalline form (solid curves)
- l- liquid form (solid line)
- all others are gases (dashed curves)



The constituents of the sublimates and gases from Mauna Ulu are thus, $\text{CaSO}_4(\text{c})$, $\text{NaSO}_4(\text{c})$, $\text{CaSO}_4(\text{c})$, $\text{SiO}_2(\text{c})$, $\text{H}_2\text{SO}_4(\ell)$, $\text{SO}_2(\text{g})$, $\text{HCl}(\text{g})$ and $\text{HF}(\text{g})$.

The data from all volcanic gas and sublimate information may be used to aid in the estimation of the conditions occurring on Mauna Ulu in March 1982.

CHAPTER VI - SUMMARY OF CONCLUSIONS:

(6.1) Summary

(1) X-ray diffraction methods yield very high background levels indicating an amorphous major phase.

(2) Major element analyses provide that SiO_2 and TiO_2 increase with alteration. Samples high in brown altered material are rich in Fe_2O_3 (total iron) and Al_2O_3 . Samples high in amorphous material are rich in SiO_2 and Fe_2O_3 (total iron).

(3) CIPW norms show that altered samples are high in normative quartz and lower in orthoclase, albite, anorthite than in fresh samples. Olivine is absent in altered samples. Normative corundum is common only in altered samples.

(4) Composition - volume calculations determine that in the alteration reaction SiO_2 is the most reactive. Fe_2O_3 , Al_2O_3 , MgO , CaO are also reactive in the alteration process. TiO_2 and Na_2O are slightly reactive while K_2O , MnO , P_2O_5 are not involved in the reaction process at all.

(5) 0.14% SO_2 was determined in one altered sample by a sulphur titration method. The occurrence of bright yellow powder also indicates pure sulphur may be present. Oxidation prevalence supports the probability of sulphate occurrence.

(6) The volcanic gases of Mauna Ulu consist mostly of air and water. As distance from fumarole increases, Po_2 increases and temperature decreases; thus components become oxidized as the gas cools. At higher temperatures (400°C) halides are

dominant, while at lower temperatures. (400°C), sulphates dominate. H_2S is common at very high temperatures but becomes rapidly oxidized to SO_2 .

From these conclusions, using the chemical and physical evidence determined in this thesis, and the type of gases found at Mauna Ulu; a table of probable mineral species has developed (Table 6.1.1). The major alteration phase is opaline silica. Other species are hematite and sulphur, with minor halides, sulphates and chlorite.

The alteration is an oxidation process, occurring by the constant reaction of basaltic lava with volcanic gases. Changing temperatures, oxidation states and acidity result in acid alteration of the lava. The alteration products are complex, yet distinctively brightly coloured.

(6.2)- Suggestions for Further Work

The work done for this thesis has been very broad and general. Time and field work constraints did not allow for detailed analyses to be performed. Future work in fumarolic alteration on Mauna Ulu should include extensive sampling of volcanic gases, their temperatures, condensates and altered materials. Laboratory analysis would thus encompass gas analyses, trace element studies, extensive x-ray diffraction and scanning electron microscope work, to provide more detailed information. All work could then be extended to fumarolic alterations on other Hawaiian volcanoes.

TABLE 6.1.1 : Possible Alteration Products on
Mauna Ulu¹

Temp. (°C)	Colour	Chemical Evidence	Possible Occurring Minerals
150-300	Brown	Fe-rich + O ₂ + (Cl + F + NH ₄ ⁺ + B)	Fe ₂ O ₃ (Hematite) [FeCl ₂ (lawrencite)] [NH ₄ Cl (salammoniac)]
	White	Al-rich + O ₂ + (Cl + F + NH ₄ ⁺ + B) + (Ca + Mg + Na)	AlCl ₃ ·6H ₂ O (chloroaluminate) NaMgAl(F,OH)·H ₂ O (ralstonite) NaCl (Halite) CaF ₂ (fluorite) [(Mg,Al,Fe) ₆ (Si,Al) ₄ O ₁₀ (OH) ₈] (green) (chlorite)
-100	Orange or Yellow	Si-rich + O ₂ + Fe	SiO ₂ (amorphous opaline silica) Fe ₂ O ₃ (hematite)
	Yellow or White	S + O ₂ + (Na+Ca+Mg+Al)	S (sulphur) [Na ₂ SO ₄ (thenardite)] [CaSO ₄ ·2H ₂ O (gypsum ²)] [FeAl ₂ (SO ₄) ₄ ·22H ₂ O (Halotrich ³)]

1-information in square brackets indicates minor phases

2-due to H₂O-rich volcanic gases, it is doubtful that anhydrite would form.

3-evidenced in only one sample, but probably common to all.

APPENDIX A:Composition - Volume Sample Calculation:(Wright's fresh basalt) + 1(x) \longrightarrow (sample 13AA)

$$x_i = a \left[f_v \left\{ \frac{g_B}{g_A} \right\} C_1^B - C_1^A \right]$$

assume: a = 100 g

 $f_v = 1$ g (fresh basalt) = 2.772 g/cm³g (sample 13AA) = 2.860 g/cm³

- data for weight percents of components (C_i) are found in Table 4.1.1.

$$x_i = 100 \left[(1) \left(\frac{2.860}{2.772} \right) C_1^B - C_1^A \right] = 103.1746 (C_1^B - C_1^A)$$

$$X_{SiO_2} = 103.1746 (71.29 - 49.37) = 2261.59$$

$$X_{Al_2O_3} = 103.1746 (7.02 - 12.56) = -571.59$$

$$X_{Fe_2O_3} = 103.1746 (9.91 - 11.61) = -175.40$$

$$X_{MgO} = 103.1746 (6.06 - 11.03) = -512.78$$

$$X_{CaO} = 103.1746 (1.53 - 10.19) = -893.49$$

$$X_{Na_2O} = 103.1746 (0.88 - 2.10) = -125.87$$

$$X_{K_2O} = 103.1746 (0.06 - 0.42) = -37.14$$

$$X_{TiO_2} = 103.1746 (2.99 - 2.30) = 71.19$$

$$X_{MnO} = 103.1746 (0.04 - 0.18) = -14.44$$

$$X_{P_2O_5} = 103.1746 (0.21 - 0.23) = -2.06$$

Results are shown in Table 4.4.2 and Graph 4.2

REFERENCES

1. Basaltic Volcanism Study Project (1981) Basaltic Volcanism on the Terrestrial Planets; Pergamon Press Inc. pp 1286.
2. Casadevall, T.J., Greenland, L.P., (1980) The Chemistry of Gases Emanating from Mount St. Helens, May-September 1980 pp 221-226 in: Lipman, P.W., Mullineaux, D.R. (editors). The 1980 Eruptions of Mount St. Helens, Washington, Geological Survey Professional Paper 1250.
3. Clark, S.P. Jr. (editor) (1966) Handbook of Physical Constants; Geological Society of America Memoir 97, pp 587.
4. Deer, W.A., Howie, R.A., Zussman, J. (1966) An Introduction to the Rock Forming Minerals; Longman Group Ltd. pp 528.
5. Delthier, D.P., Pevear, D.R., Frank, D. (1980) Alteration of New Volcanic Deposits, pp 649-665 in: Lipman, P.W., Mullineaux, D.R. (editors) The 1980 Eruptions of Mount St. Helens, Washington; Geological Survey Professional Paper 1250.
6. Fudali, R. (1965) Oxygen Fugacities of Basaltic and Andesitic Magmas; *Geochimica et Cosmochimica Acta*, 29, 1063-1075.
7. Gerlach, T.M. (1980) Evaluation of Volcanic Gas Analyses from Kilauea Volcano; *Journal of Volcanology and Geothermal Research*, 7, 295-317.
8. Gresens, R.L. (1967) Composition - Volume Relationships of Metasomatism; *Chemical Geology*, 2, 47-65.
9. Hazlett, R.W. (1982) Guide to Points of Geologic Interest in the Kilauea Section of Hawaii Volcanoes National Park, Hawaii.
10. Hutchison, C.S. (1974) Laboratory Handbook of Petrographic Techniques, John Wiley and Sons, pp 527.
11. Keith, T.E.C., Casadevall, T.J., Johnston, D.A. (1980) Fumarole Encrustations: Occurrence, Mineralogy and Chemistry, pp 239-250 in: Lipman, P.W., Mullineaux, D.R., (editors). The 1980 Eruptions of Mount St. Helens, Washington, Geological Survey Professional Paper 1250.
12. Kerr, P.F. (1977) Optical Mineralogy, McGraw-Hill Inc. pp 492.
13. Naughton, J.J., Lewis, V.A., Hammond, D., Nishimoto, D. (1974) The Chemistry of Sublimates collected directly from Lava Fountains at Kilauea Volcano, Hawaii; *Geochimica et Cosmochimica Acta*, 38, 1679-1690.

14. Naughton, J.J., (1980) Composition of Some Components in Gas Collected during the 1977 Eruption at Kilauea, Hawaii; *Journal of Volcanology and Geothermal Research*, 7, 319-322.
15. Peterson, D.W., Christiansen, R.L., Duffield, W.A., Holcomb, R.T., Filling, R.I. (1976) Recent Activity of Kilauea Volcano, Hawaii; Proceedings of the Symposium on: "Andean and Antarctic Volcanology Problems" (Santiago, Chile, September 1974).
16. Stoiber, R.E., Rose, W.I. Jr. (1974) Fumarole Encrustations at Active Central American Volcanoes; *Geochimica et Cosmochimica Acta*, 38, 495-516.
17. Swanson, D.A., Duffield, W.A., Jackson, D.B., Peterson, D.W. (1979) Chronological Narrative of the 1969-1971 Mauna Ulu Eruption of Kilauea Volcano, Hawaii; Geological Survey Professional Paper 1056.
18. Tilley (1922) *Mineralogy Magazine*, 19, 275.
19. Wright, T.L., Swanson, D.A., Duffield, W.A. (1975) Chemical Compositions of Kilauea East-Rift Lava, 1968-1971, *Journal of Petrology*, 16, Part 1, 110-133.